# DEVELOPMENT OF MEMBRANE DISTILLATION SYSTEM POWERED BY CAR EXHAUST FOR WATER DESALINATION

BY

**Abdelrahman Etman**

A Thesis Presented to the
DEANSHIP OF GRADUATE STUDIES

**KING FAHD UNIVERSITY OF PETROLEUM & MINERALS**

DHAHRAN, SAUDI ARABIA

In Partial Fulfillment of the
Requirements for the Degree of

# MASTER OF SCIENCE

In

MECHANICAL ENGINEERING

May 2017

KING FAHD UNIVERSITY OF PETROLEUM & MINERALS

DHAHRAN- 31261, SAUDI ARABIA

**DEANSHIP OF GRADUATE STUDIES**

This thesis, written by **Abdelrahman Etman** under the direction of his thesis advisor and approved by his thesis committee, has been presented and accepted by the Dean of Graduate Studies, in partial fulfillment of the requirements for the degree of **MASTER OF SCIENCE IN MECHANICAL ENGINEERING.**

A. Khalifa

Dr. Atia Khalifa
(Advisor)

Dr. Zuhair Gasem
Department Chairman

Dr. Mohammed Antar
(Member)

Dr. Salam A. Zummo
Dean of Graduate Studies

17/10/11.7

***Date***

Med Habib

Dr. Mohammed Habib
(Member)



II

**I dedicate this work to my dear family**

# ACKNOWLEDGMENTS

I want to say thank you to my family in Egypt, King Fahd University and the Mechanical engineering department, my advisor and big brother Dr. Atia Khalifa, my supporting committee members Dr. Antar and Dr. Habib, mechanical engineering lab supervisor Mr. Karam who helped me a lot through my experimental work, my Sudanese friend Mr. Mohamed Aly, Egyptian community at KFUPM and all my friends and colleagues who stood beside me through this journey.

## List of Contents

# List of figures

# List of tables

# Abstract

Full Name : [Abdelrahman Abdelsalam Tawfik Etman]

Thesis Title : [DEVELOPMENT OF MEMBRANE DISTILLATION SYSTEM POWERED BY CAR EXHAUST FOR WATER DESALINATION]

Major Field : [Mechanical Engineering]

Date of Degree : [October 2017]

The World nowadays faces a severe potable water rareness issues in many countries in additon to high energy consumptions and environmental considerations. In order to face these problems, many scientists all over the world have conducted extensive research in the field of renewable energy desalination techniques. In this thesis, we aimed to examine the possibility of using car engine exhaust gases to heat the feed water of a membrane distillation module. Throughout this work, we have carried out many studies to cover this topic from almost all its aspects. A numerical design and fabrication of a suitable heat exchanger was the first task to be handled. Experiments were done in the lab using a lab engine equipped with all the necessary tools to test the effect of all variables on system's parameters. Also, to obtain the second law efficiency of the system and to know which parts are responsible for most of exergy destructions, an exergy analysis was executed. Finally, we performed an economic study of the system to evaluate its feasibility. The distillate flux was found to increase with increasing engine load and speed, however, increasing engine load had more significant effect on distillate flux than increasing engine speed. It was found that the proposed system showed a very good potential to achieve its objectives. The results also showed that the heat exchanger alone was responsible for about 90% of the

destructed exergy. The second low efficiency or exergy efficiency was found to increase with increasing feed water temperature. Finally, the cost of the unit production was found to be 3.71 $\$/m^3$. It was also found that reducing the membrane replacement cost and increasing system life time had a significant positive effect on water production cost.

# ملخص الرسالة

**الاسم الكامل: عبد الرحمن عبد السلام توفيق عتمان**

**عنوان الرسالة: تطوير وحدة تحلية مياه غشائية يتم تزويدها بالطاقة عن طريق عادم محرك سيارة**

**التخصص: الهندسة الميكانيكية**

**تاريخ الدرجة العلمية: اكتوبر 2017**

إن العالم اليوم يواجه تحديات صعبة فيما يخص توافر المياه الصالحة للشرب في كثير من البلدان، بالإضافة إلى تحديات التقليل من استهلاك مصادر الطاقة وأيضا التغيرات المناخية التي باتت تشكل خطرا على البشرية كلها. يقوم العلماء على مستوى العالم بإجراء الكثير من البحوث لمواجهة تلك التحديات من خلال التقنيات الحديثة لتنقية المياه باستخدام الطاقة المتجددة. الهدف من تلك الرسالة كان معرفة الى أي مدى يمكن استخدام عادم السيارة لتسخين المياه المغذية لوحدة التحلية من نوع الغشاء التقطيري. خلال العمل بالرسالة تم تغطية الموضوع من جميع الجوانب تقريبا. كانت أولى خطوات المشروع هي تصميم مبادل حراري مناسب لاحتياجنا ومن ثم تصنيعه. بعد ذلك تم اجراء تجارب معملية باستخدام محرك بنزين بالمعمل لمعرفة مدى تأثير المتغيرات المختلفة على أداء وحدة التحلية. كما تم عمل دراسة للنظام ككل معتمدة على القانون الثاني للديناميكا الحرارية لمعرفة كفاءة النظام وأي الأجزاء بالتحديد تحتاج الى التحسين أكثر من غيرها. وأخيرا قمنا بإجراء دراسة اقتصادية للنظام لمعرفة تكلفة تنقية المياه من خلاله وكذلك لدراسة جدوى استخدامه. في النهاية، فإن النظام المقترح قد أبدى قدرة جيدة جدا على تنفيذ المهمة التي تم تصميمه من أجلها.

# Chapter 1: Introduction and literature

## 1.1 Introduction

As the population grows all over the world, the need for new fresh water resources also increases. Since the natural fresh water resources are limited and consumed in a higher rate than ever [1] & [2], there is an urgent need for new sea water and brackish water desalination techniques. These techniques should be energy and cost efficient to provide the pure water in a reasonable price.

The Arab world and especially the Gulf countries face a relatively bigger water scarcity problem than other world regions, while they have access to sea water [3] & [4]. This led to a persistent need for sea water desalination techniques that can supply increasing fresh water demand and in the same time they should be energy efficient.

Membrane distillation (MD) [5] & [6] is a very promising way of producing pure water because of its many attractive features such as it has a low operating pressure and temperature, reasonable high productivity and high product quality.

The aim of this thesis is to study water desalination using a membrane distillation unit powered by engine exhaust from many aspects. During the literature review many papers were read. This literature covers desalination in general and then focus on MD technique from many aspects, such as MD theory of operation, main features, advantages and drawbacks, different

configurations, governing equations, effect of operating conditions, using waste and renewable energies with MD, exergy analysis and the economic aspect of MD.

### 1.2. literature review

#### 1.2.1 Desalination

Industrial water desalination [7] to [11] techniques are classified into two main categories [12]:

- Thermal desalination, where water is evaporated and then condensate to get rid of salts. such as: Multi-stage flash (MSF), Multi-effect Distillation (MED) and Vapor compression distillation (VCD.) They have the advantages of less operational and maintenance costs compared to other techniques and less energy consumption for low operating temperature plants.
- Membrane desalination, where brackish water is forced to pass through the bores of a membrane that allows only water molecules and blocks salts. such as: Reverse osmosis (RO) and Nano filtration (NF.) they have the advantages of less power consumption because there is no phase change, compact, and easy to maintain. While the limitations are that they need pretreatment and they are not suitable for concentrated solutions. due to these drawbacks, finding a new water desalination technique has become essential.

There are some emerging water desalination techniques, such as [13]: Forward osmosis, Dew evaporation, Membrane distillation, Nano-desalination, Thermo-ionic desalination, Low temperature thermal desalination, Capacitive deionization, Solar desalination and Geothermal desalination.

### 1.2.2 Membrane distillation

Membrane distillation (MD) is a thermally-driven membrane separation technology for separating water vapor from feed water solution. In membrane distillation, a hot saline feed stream is passed over a micro-porous hydrophobic membrane. The temperature difference between the two sides of the membrane leads to a vapor pressure difference that causes water vapor in the hot feed side to pass through the membrane pores, and condense either on the cold side of the membrane, or in an external condenser.

Alkhudhiri et al [16] and others [17] to [22] made a comprehensive review for the MD. They defined the MD as a thermally-driven separation process, in which only vapor molecules transfer through a microporous hydrophobic membrane. The force driving the MD process is the difference of the vapor pressure which is a result of temperature difference between the two sides of the hydrophobic membrane.

**Advantages** of the MD:

- Low operating temperature (low energy consumption)
- Low operating pressure
- Less demanding membrane characteristics
- Suffers less from fouling
- Can use solar or waste heat
- High product quality (salt rejection is almost 100%)

While the **drawbacks** are:

- Susceptible permeate to temperature and concentration polarization effect.

- High conduction heat losses in membrane.

The MD systems have **four configurations**:

**1. Direct Contact Membrane Distillation (DCMD)**

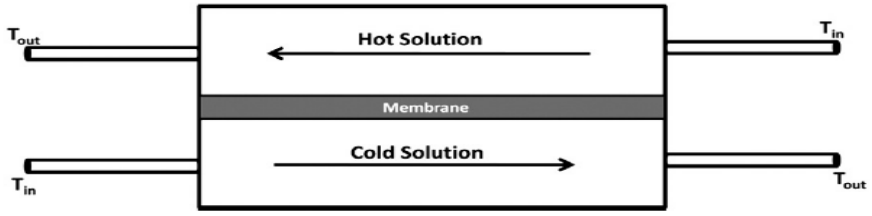


*Figure 1-1 DCMD*

In direct contact MD, the hot solution (feed) and the cold permeate are in direct contact with sides surfaces of the membrane. This configuration is simple and it is widely used in water desalination and other applications like manufacturing of acids. The disadvantage of DCMD is the high heat loss by conduction.

**2. Air Gap Membrane Distillation (AGMD)**

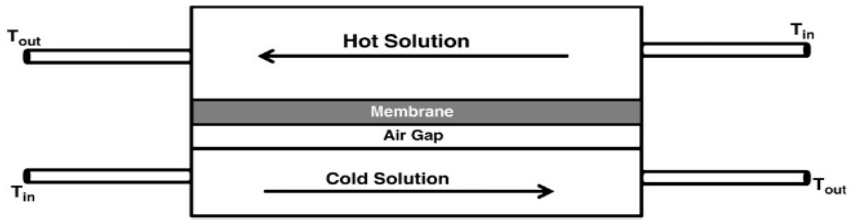


*Figure 1-2* ***AGMD***

In air gap MD, feed solution is in direct contact with the hotter surface of the membrane only, while stagnant air exists between both the condensation surface and the membrane. And it is the type used in this work. the advantage of this AGMD is the lower heat losses compared to DCMD. While it's drawback is higher mass transfer resistance. And it is used in water desalination and removing volatile compounds from aqueous solutions.

**3. Sweeping Gas Membrane Distillation (SGMD)**

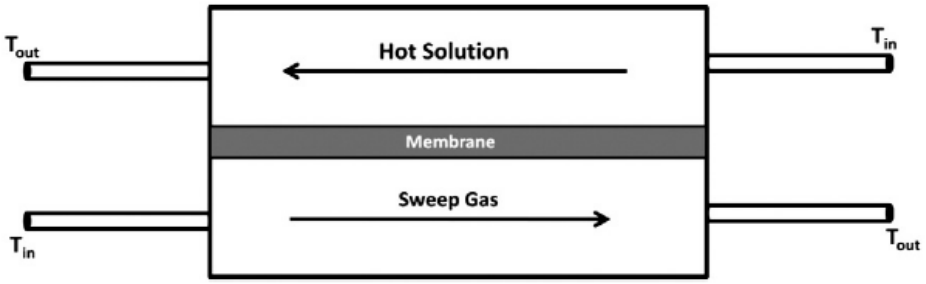


*Figure 1-3* ***SGMD***

Here the vapor at the permeate membrane side is swept using an inert gas, so that the vapor condensates outside the membrane module. Like AGMD, SGMD has less heat losses but it also

has lower mass transfer resistance when compared to AGMD. And it is also used in removing volatile compounds from aqueous solutions.

**4. Vacuum Membrane Distillation (VMD)**

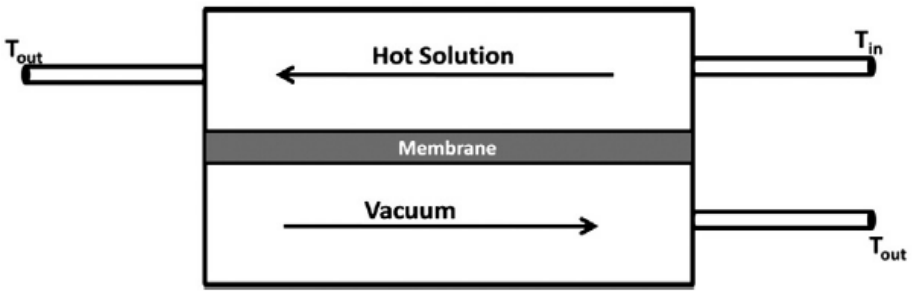


*Figure 1-4* ***VMD***

A pump is used in VMD configuration, to vacuum the permeate side of the membrane, while the vapor condensates outside the membrane module. Here, the heat lost by conduction is considered negligible.

**MD power resources**

As the MD works at lower temperatures compared to other thermal desalination techniques (40 to 90 °C), renewable energy resources and waste heat can be used to power MD systems, in addition to conventional heating.

Rasool et al [23] reviewed the efforts of researchers in the field of solar powered membrane distillation. Hogan et al. [24] had the first publication in this field. They used solar collectors with an area of 3 m2 to power a 0.05 m3 /day system. They reported 55.6 kWh/m3 energy consumption, and a flux of approximately 17 liters/day m2. Thomas [25] reported a membrane

distillation system powered by solar energy. A 12 m2 of vacuum tube collectors and a flat plate module were used. The plant had a 40 l/hour maximum flux.

Xu et al. [26] tested the performance of VMD unit for desalination of sea water on a vessel, with feed seawater heated using waste heat of the engine of the ship. They obtained a membrane flux of 5.4 kg/m2 h and a salt rejection factor of 99.99% at –0.093 Mpa and 55°C.

Khalifa et al. [27] used electric heating to study the performance of an AGMD unit. A 7.25 kW electric heater was used to heat the feed water before it enters the membrane cell. Using experimental and theoretical studies, they reported the effect of MD system operating conditions on the permeate flux.

**Waste energy powered desalination**

The need for energy efficient water desalination techniques is very essential. Low grade energy can be used to power desalination units with relatively low operating temperatures such as membrane distillation. Chunhua [28], et al studied Multi effect desalination system MED powered by waste hot water from petrochemical industry with a production capacity of 10,000 m3/d. Results showed that every 1 °C increment in feed water temperature would increase the output of freshwater by approximately 438 m3/d. Also, the operating cost of their system was found to be 39.5% lower than that of system running by steam. Dastgerdi et al [29], developed a new distributed boosted multi-effect distillation (DBMED) process to effectively harness low-grade “waste heat” in the temperature range 65 °C–90 °C. they achieved up to 38% reduction in normalized pumping power consumption NPPC at 90 °C. Lokare et al [30] studied a DCMD powered by exhaust stream from Natural

Gas Compressor Station NG CS in Pennsylvania. The key findings of this study suggest that DCMD can concentrate all the produced water in PA if the waste heat from NG CS can be utilized.

**Membrane characterizations**

Membranes used in the MD process are non-wetting (Hydrophobic) microporous membranes. These membranes should be having less mass transfer resistance and less thermal conductivity to decrease heat losses in the membrane. Membranes should also have high resistance to chemicals and high thermal stability to withstand extreme temperatures. The following are some features that are used to describe a certain membrane:

- Membrane thickness: thicker membrane yields lower permeate and lower losses, so it has to be optimized. (30-60 microns)

- Contact angle: it is a measure of membrane hydrophobicity (above 90 degrees for hydrophobic membranes)

- Membrane material: common materials are: PTFE & PVDF.

- Pore size: larger pore size yields higher permeate, but very large pore size may cause membrane wetting. (0.1-1 microns)

- LEP (liquid entry pressure): it is the maximum pressure limit after which liquid may pass the membrane causing membrane wetting. It depends on two major parameters which are pore size and hydrophobicity of the membrane.

- Porosity: it is the ratio between volume of the holes in the membrane and the membrane total volume. Where higher porosity yields higher permeate and lower conduction losses.

- Tortuosity: it is a measure of the deviation of pores from cylindrical shape.

**Effect of operating parameters on the performance of DCMD**

Shirazi et al. [31] and Schofield et al. [32] studied the performance of a DCMD system. Investigated variables included feed temperature, feed-permeate temperature difference and ratio, feed flow rate, permeate flow rate, feed-permeate flow rate ratio, feed concentration, membrane pore size, cold permeate temperature and membrane degradation with time.

Following observations were obtained:

1. When the feed temperature increases, permeate flux also increases, almost in an exponential way.
2. The flux increases as the cold permeate temperature decreases. When permeate temperature decreases, it causes the transmembrane vapor pressure difference to increase; which leads to increasing the permeate flux.
3. As temperature difference increases, the flux also increases. However, at a given temperature difference, higher cold permeate temperature yields higher flux. This may be because large conduction heat loss across the membrane and from the module itself to the surroundings at lower temperature of the cold permeate stream.
4. Flux increases exponentially as the temperature ratio increases.

5. The flux increases prominently as feed flow rate increases.
6. Permeate flux increases as the flow rate of the cold permeate stream increases.
7. The flux increases in a parabolic manner as the flow rate ratio increases.
8. Permeate flux is continuously decreasing as the feed salinity increases.

**Effect of operating conditions on the performance of an AGMD**

Khalifa et al [33] studied the performance AGMD system. They investigated the effect of the AGMD operating parameters such as feed flow rate, feed inlet temperature, coolant flow rate, coolant temperature, membrane pore size, air gap width and the feed concentration on the permeate flux.

The results were as follows:

1. As the feed temperature increases, permeate flux rises exponentially.
2. The flux is directly proportional to the feed flow rate.
3. When the coolant flow rate increases, there is an insignificant change in flux.
4. Mass transfer resistance is directly proportional to air gap width.
5. The permeate flux of the PTFE 0.22µm membrane is slightly less compared to the permeate flux of the PTFE 0.45µm membrane.
6. As the feed concentration increases, gradual decrease in permeate flux rate occurs.
7. Permeate flux is almost constant during the first 12 hours of the experiment. The permeate flux then starts to gradually drop until the experiment ends.

8. The permeate TDS (total dissolved solids) increases with time, but still good.

## Performance of SI engine

Khalifa et al. [34] carried out a theoretical and experimental study to compare the effects of using octane 95 and octane 91 on the performance of SI engine. For engine speeds less than 3500 rpm, results showed that there are no big differences between engine performances in both cases. It was found that fuel consumption is slightly less for engine operating with octane 91. The exhaust gas temperature doesn't change significantly with changing the fuel type as shown in figure 1.5.

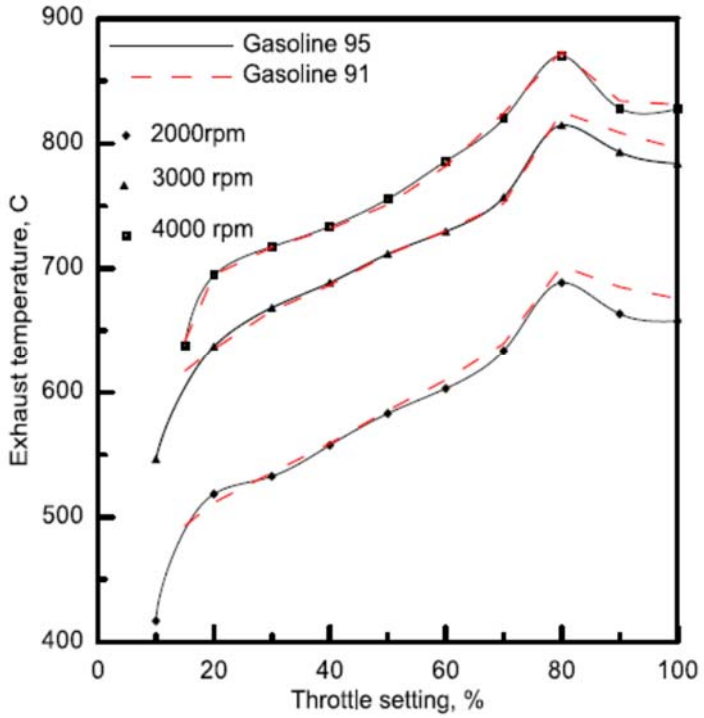


*Figure 1-5* ***Comparing exhaust gas temperatures for 95 and octane 91 fuels***

**Thesis Objectives, methodology and expected outcomes:**

**Objectives:**

The main objective of this thesis is to study the performance of an MD system that is powered by the waste heat of engine exhaust, at different loads and speeds of the engine.

Thesis work includes the following experimental and analytical tasks:

1. MD module design, fabrication and testing

2. Heat exchanger design, fabrication, installation, and testing

3. Attaching the heat exchanger and the MD module to the engine exhaust system

4. studying the effects of engine load and speed

5. Revising the heat exchanger design and performance to achieve feed temperature of 70C and above, if possible.

6. Experimental investigation of MD system operating conditions (Feed and coolant flow rates, coolant temperatures, etc.)

7. Exergy analysis of the proposed MD system

8. Economic analysis of the proposed MD system

**Methodology:**

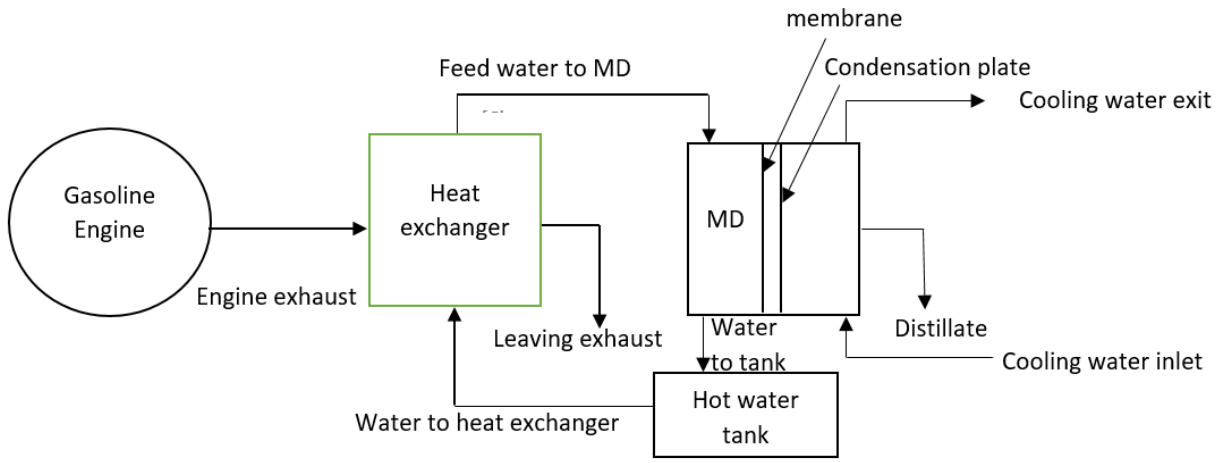


*Figure 1-6* ***lay out of the proposed system***

To achieve above objectives, an IC lab engine equipped with necessary tools was used, also a suitable heat exchanger was designed, fabricated and attached to the engine exhaust pipe, also. An air gab MD module was used to complete main parts of the experimental setup. A set of experiments was carried out in the lab in order to assess the effects of different parameters on the AGMD performance. An exergy analysis was done to obtain the second law efficiency of the system, and to figure out the main parts responsible for exergy losses. Finally, an economic study was performed to assess the feasibility of the proposed system.

**Expected outcomes:**

The expected outcomes of this work are:

1. A full set of experimental results that evaluates the proposed system through showing the effect of different variables on the performance of the system.
2. An EES code that helps doing a full exergy analysis for the system.
3. An Economic study of the system.

# Chapter 2: Heat exchanger design and fabrication

## 2.1 Introduction

The aim of this chapter is to highlight the efforts done during the process of designing the heat exchanger used in the experimental setup. The deign process goal was to achieve the most possible heat transfer between engine exhaust and input water to the MD module within limits.

The design process consisted of two phases. Phase one is the numerical design, and phase two is the practical execution of the chosen heat exchanger design.

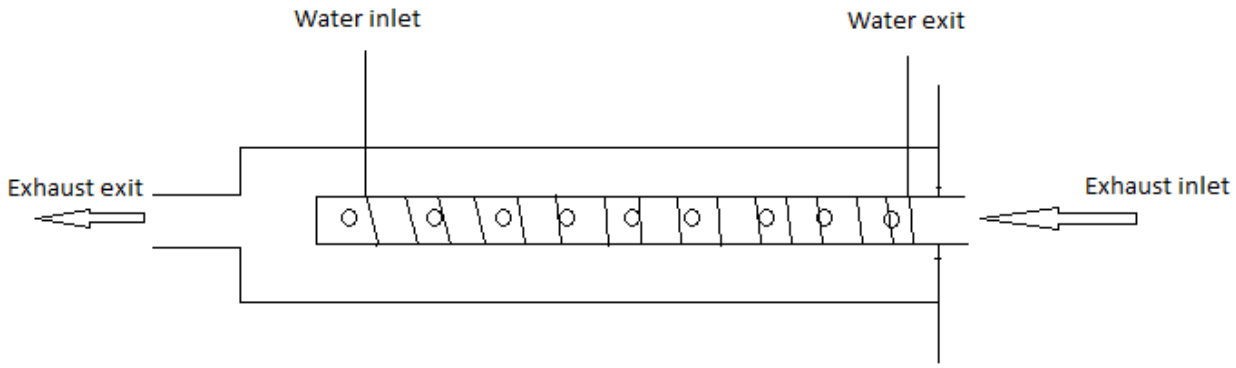


*Figure 2-1 Water and exhaust inlets and exits from the heat exchanger*

The EES software was used to generate the analytical code and design calculation of the heat exchanger. While the practical execution of the heat exchanger passed through many steps and modifications at the university workshop and outside. The heat exchanger consists of an inner tube with holes and a copper coil wound around it, and the outer casing. Exhaust gases flow through the inner tube and out from the holes transferring its heat to the water flowing through the coil.

## 2.2 Analytical design

The Effectiveness–NTU Method was applied for heat exchanger design. Here we will be trying to find out the length of the coil tube, while other data are given or controlled, based on the actual design.

Givens:

$\dot{m}_{water}$ : water mass flow rate [kg/s]

$T_{Win}$ : water inlet temperature to the heat exchanger [C]

$T_{Exh\ in}$ : exhaust inlet temperature to the heat exchanger [C]

rpm: engine speed [rpm]

$D_{coil\ inner}$: coil tube inner diameter [m]

$D_{coil\ outer}$ : coil pipe outer diameter [m]

$D_{coil\ wound}$: diameter of the wound coil [m]

$D_{outer\ box}$ : shell hydraulic diameter [m]

t: coil thickness [m]

$Cp_{Water}$ : water specific heat [Kj/Kg.k]

$\rho_{air}$: air density [Kg/$m^3$]

$V_{displaced}$ : engine displaced volume [$m^3$]

$\eta_{vol}$ : engine volumetric efficiency [%]

$Cp_{exhaust}$ : engine exhaust specific heat [Kj/Kg.k]

$\mu_{water}$ : water viscosity [Pa.S]

$\mu_{exhaust}$ : exhaust viscosity [Pa.S]

$Pr_{water}$ : water Prandtl number

$Pr_{exhaust}$ : exhaust Prandtl number

$K_{water}$ : water thermal conductivity [W/m.K]

$K_{exhaust}$ : exhaust thermal conductivity [W/m.K]

**Methodology**

Heat gained by water is

$$Q = \dot{m}_{water} * Cp_{Water} * (T_{Wout} - T_{Win})$$

While Water heat capacity is

$$C_{water} = \dot{m}_{water} * Cp_{Water}$$

For 4-stroke car engine, air flow rate is

$$m_{air} = \rho_{air} * V_{displaced} * rpm * \eta_{vol} / (4 * 60)$$

And assuming air to fuel ratio of 14:1, hence, exhaust flow rate is

$$\dot{m}_{exhaust} = 1.0667 * m_{air}$$

And, the exhaust heat capacity is

$$C_{exhaust} = \dot{m}_{exhaust} * Cp_{exhaust}$$

From energy balance

$$C_{exhaust} * (T_{exhaust\ in} - T_{exhaust\ out}) = C_{water} * (T_{Wout} - T_{Win})$$

And the effectiveness of the heat exchanger is

$$\epsilon = Q / Q_{max}$$

$$Q = \dot{m}_{water} * Cp_{Water} * (T_{Wout} - T_{Win})$$

$$Q_{max} = C_{min} * (T_{exhaust\ in} - T_{Win})$$

$$\text{NTU} = \left(-\frac{1}{C_r}\right) * \ln(C_r * \ln(1\text{-}\epsilon) + 1)$$

$$C_r = C_{min}/C_{max}$$

where

$$Q_{max} = C_{min} * (T_{exhaust\ in} - T_{Win})$$

Where $C_{min}$ is the minimum heat capacity between $C_{exhaust}$ & $C_{water}$, and capacity ratio is

$$C_r = C_{min}/C_{max}$$

The Number of Transfer Units (NTU) for a cross flow heat exchanger is:

$$\text{NTU} = \left(-\frac{1}{C_r}\right) * \ln(C_r * \ln(1\text{-}\epsilon) + 1)$$

Neglecting the pipe length, the overall heat transfer coefficient is

$$\text{U} = \frac{1}{\left(\frac{1}{h_i}\right) + \left(\frac{1}{h_o}\right)}$$

Where $h_i$ & $h_o$ are the internal and outer convection heat transfer coefficients respectively.

For water inside the coil, Reynolds number is

$$Re_{internal} = 4 * \frac{m_{water}}{\pi * D_{coil\ inner} * \mu_{water}}$$

According to Reynolds number, the flow is said to be turbulent or laminar. For turbulent flow, the Nusselt number is

$$Nu_{internal} = 0.023 * Re_{internal}^{0.8} * Pr_{water}^{0.4}$$

While for laminar flow, assuming constant heat flux, the Nusselt number is equal to 4.36

Also

$$Nu_{internal} = h_i * \frac{D_{coil\ inner}}{K_{water}}$$

For exhaust outside the coil

$$D_{hydraulic} = D_{shell} - D_{coil\ wound}$$

And

$$Re_{external} = 4 * \frac{m_{exhaust} * D_{hydraulic}}{\pi * (D_{shell}^2 - D_{coil\ outer}^2) * \mu_{exhaust}}$$

The average heat transfer coefficient for cross-flow over a cylinder can be found from the correlation presented by Churchill and Bernstein

$$Nu_{external} = 0.3 + (0.62*Re_{external}^{0.5} * Pr_{exhaust}^{0.333}) * (1 +(Re_{external}/282000)\text{^}0.625)\text{^}0.8/$$

$$(1 + (0.4*Pr_{exhaust})\text{^}0.667)\text{^}0.25$$

And

$$Nu_{external} = h_o * \frac{D_{coil\ outer}}{K_{exhaust}}$$

From the Effectiveness–NTU Method, the heat transfer area is

$$A = NTU * \frac{C_{min}}{U}$$

And coil length is found from

$$L = \frac{A}{3.14 * D_{coil\ outer}}$$

**Sample calculations**

The following are sample calculations based on the above strategy of calculating the tube coil length and using the following practically obtained and theoretical data.

**Given data**

$\dot{m}_{water}$ : water flow rate = 2 [l/min]

$T_{Win}$ : water inlet temperature to the heat exchanger = 25 [°C]

$T_{Wout}$ : water outlet temperature from the heat exchanger = 75 [°C]

$T_{Exh\ in}$ : exhaust inlet temperature to the heat exchanger = 580 [°C]

rpm: engine speed = 2000 [rpm]

$D_{coil\ inner}$: coil pipe inner diameter = 9.5 [mm]

$D_{coil\ outer}$ : coil pipe outer diameter = 10.5 [mm]

$D_{coil\ wound}$: diameter of the wound coil = 11 [cm]

$D_{outer\ box}$ : outer box hydraulic diameter = 20 [cm]

$Cp_{Water}$ : water specific heat = 4.18 [Kj/Kg.k]

$\rho_{air}$: air density = 1.2 [Kg/$m^3$]

$V_{displaced}$ : engine displaced volume = 2000 [$CC$]

$\eta_{vol}$ : engine volumetric efficiency = 97 [%]

$Cp_{exhaust}$ : engine exhaust specific heat = 1.051 [Kj/Kg.k]

$\mu_{water}$ : water viscosity = 0.000547 [Pa.S]

$\mu_{exhaust}$ : exhaust viscosity = 0.00003 [Pa.S]

$Pr_{water}$ : water prandtl number = 3.6

$Pr_{exhaust}$ : exhaust prandtl number = 0.69

$K_{water}$ : water thermal conductivity = 0.625 [W/m.K]

$K_{exhaust}$ : exhaust thermal conductivity = 0.035 [W/m.K]

**EES code Results**

Heat transfer area = 0.216 [$m^2$]

Overall heat transfer coefficient = 81.32 [W/$m^2$C]

Pipe length = 6.879 [m]

Based on these calculations, a 3/8-inch tube coil with 7 meters' length was practically used inside the heat exchanger to achieve the required heat transfer.

Figure 2.2 shows the effect of feed water mass flow rate variation on the required tube coil length for the above conditions. As the feed water mass flow rate increases, the required tube coil length also increase. Figure 2.3 indicates that the required tube coil length is inversely proportional with the temperature of the incoming exhaust.

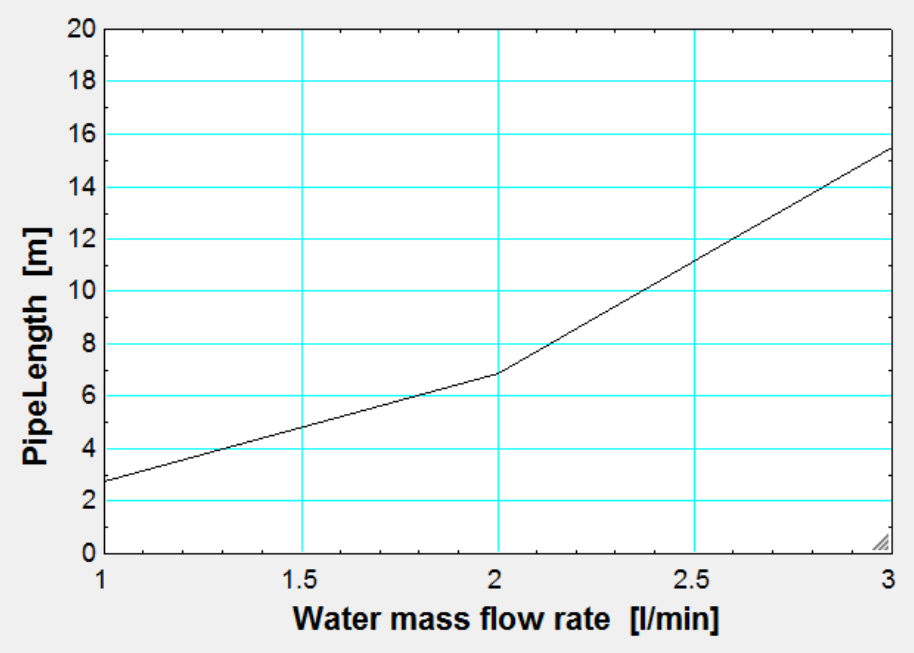


*Figure 2-2 Variation of the required tube coil length (that achieves 75 °C water exit temperature) with water mass flow rate.*

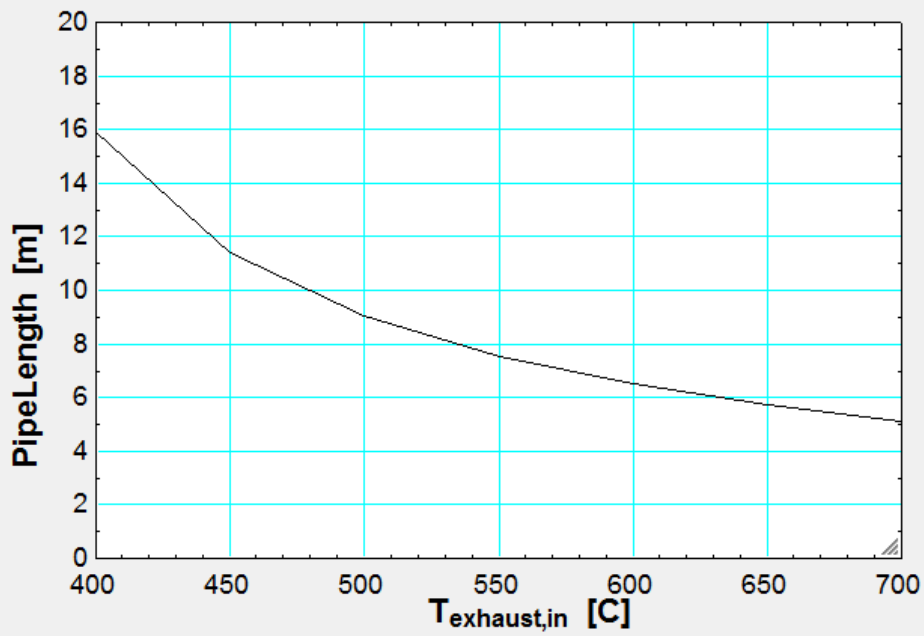


*Figure 2-3 Variation of the required tube length with the inlet exhaust temperature.*

Figures 2.4, 2.5 and 2.6 show the effect of water inlet temperature, water mass flow rate and exhaust inlet temperature on water exit temperature from the heat exchanger. Figure 2.4 and 2.6 show that water exit temperature increases almost linearly as the water inlet temperature and exhaust inlet temperature increase, while figure 2.5 shows that water exit temperature decreases as the water mass flow rate increases.

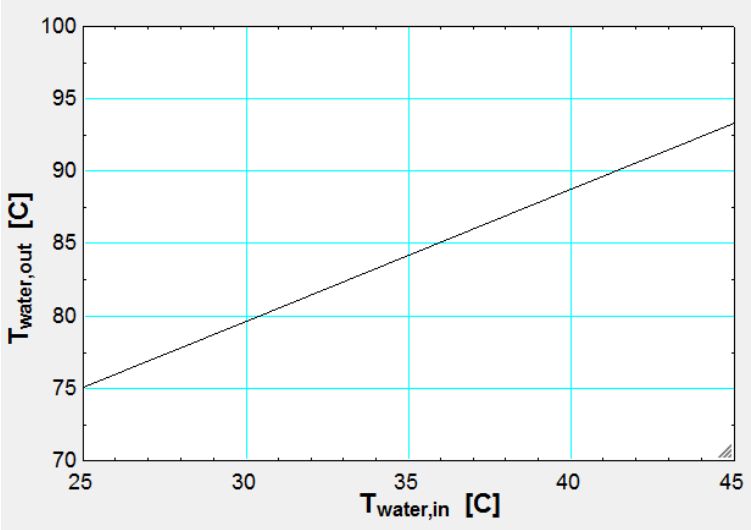


*Figure 2-4 Effect of inlet water temperature variation on water exit temperature.*

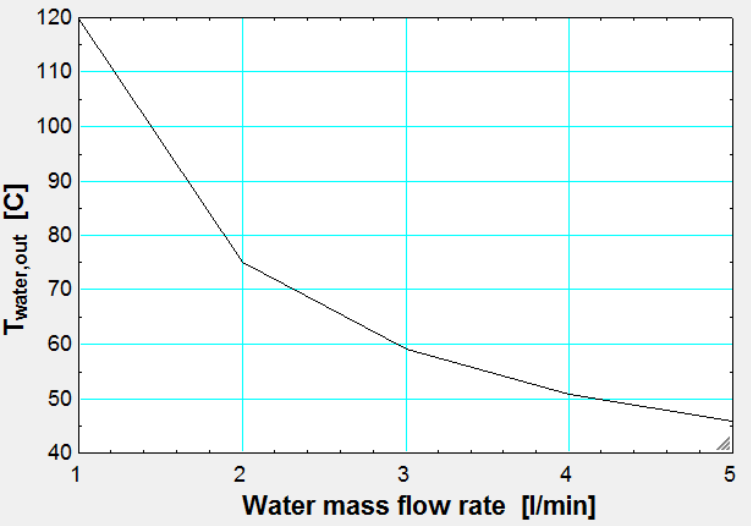


*Figure 2-5 Effect of water mass flow rate variation on water exit temperature at 2000 rpm, 25 °C inlet water temperature and 580 °C exhaust temperature.*

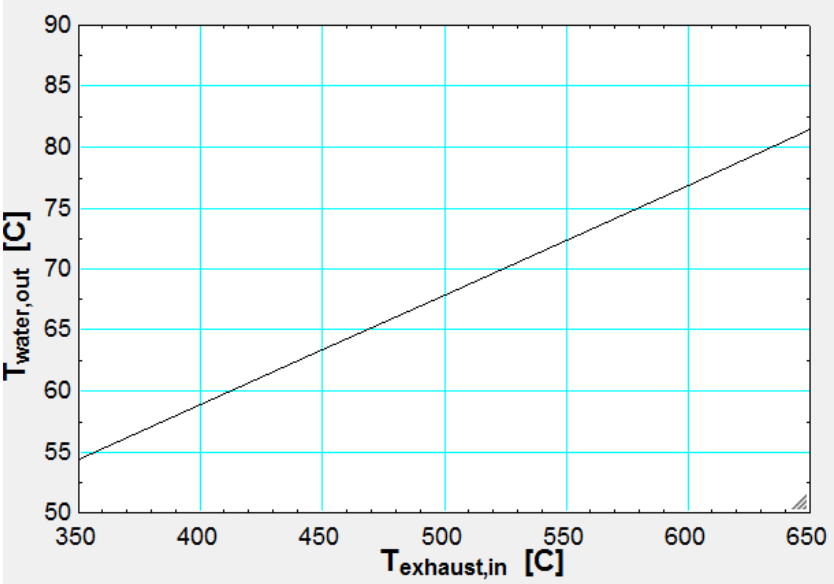


*Figure 2-6 Effect of exhaust inlet temperature on water exit temperature.*

### 2.3 Heat exchanger fabrication

Heat transfer in this heat exchanger takes place through conduction and convection. As exhaust gases flow through the inner pipe, the water flowing through the outer coil absorbs the exhaust

heat by conduction through pipes walls. Also, heat is transferred to water from exhaust gases by convection as the gases flows through the inner pipe holes and transfer its heat to the copper coil and then heat is transferred again by convection from coil to water flowing through it. The heat exchanger fabrication process passed through many modifications. the first approach, shown in figures 2.7 to 2.10, consisted of two concentric tubes with a coil wound on the internal tube. The exhaust enters the internal tube and exits from the tube holes heating the water passing through the coil.

This heat exchanger achieved high outlet water temperatures but at low water flow rate. Also, water flow rate was very low because of the small diameter of the heat exchanger coil, with a maximum flow rate of 1.5 liter/min due to the limitations of coil diameter causing head losses and no pump was used as water was drowned directly from source. figure 2.11 shows the change of outlet water temperature with the engine speed at water flow rate of 1.5 liter/min, when using this first heat exchanger.

*Figure 2-7 Inner pipe of the first heat exchanger*

*Figure 2-8 The copper coil wound on the inner pipe*

*Figure 2-9 Assembled heat exchanger*

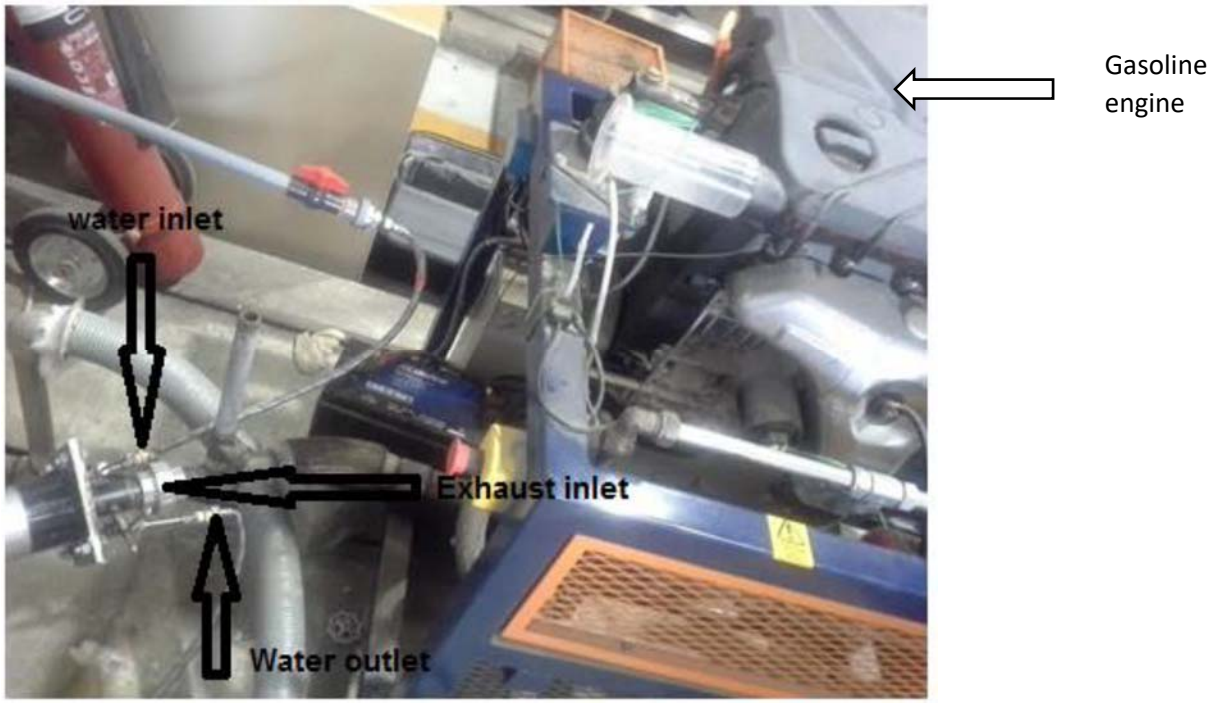


*Figure 2-10 Water inlet, water outlet and exhaust inlet to the heat exchanger attached to an engine*

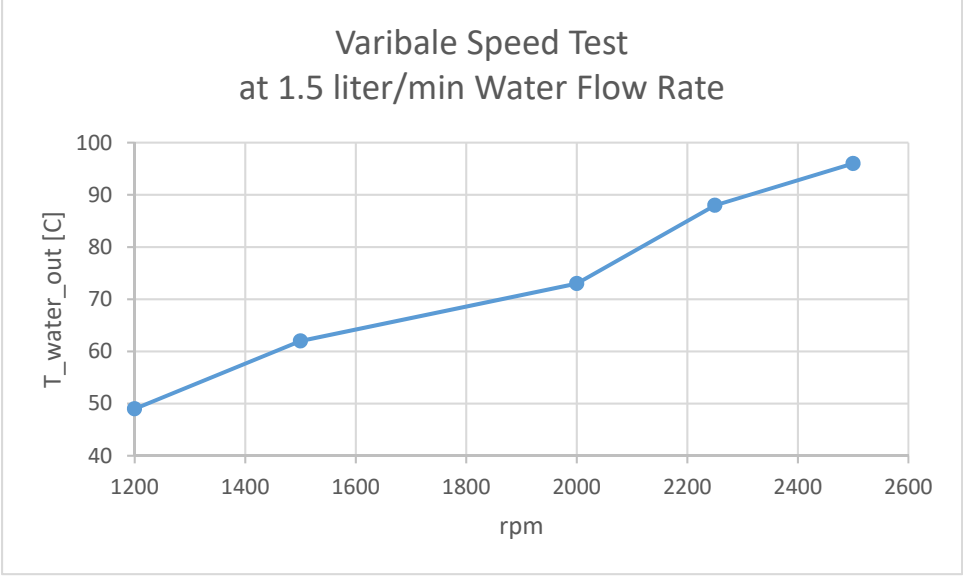


*Figure 2-11 Change of outlet water temperature with engine speed at water flow rate of 1.5 liter/min.*

## Modifications of the design

The aim of the first modification was solving the problem of low water flow rate. We removed the internal pipe and put 0.5-inch tube coil instead of the 0.25-inch tube coil that was used before and caused high friction and low water flow rate, so, the heat transfer between water and exhaust was only by convection. This modification resulted in higher flow rates of water as planned and up to 10 litre/min, but at the expense of lower exit water outlet temperatures. Now we are in a need for a heat exchanger that achieve required outlet water temperatures and at the same time allows reasonable water flow rates.

We started fabricating a new heat exchanger. 3/8-inch in diameter tube coil is used to allow higher water flow rates. We replaced the outer cylindrical casing with a bigger square one to allow more residence time. Also, we used a larger internal diameter tube in order to fit the new larger coil. Solid works software was used to design the new heat exchanger as shown in figure 2.12.

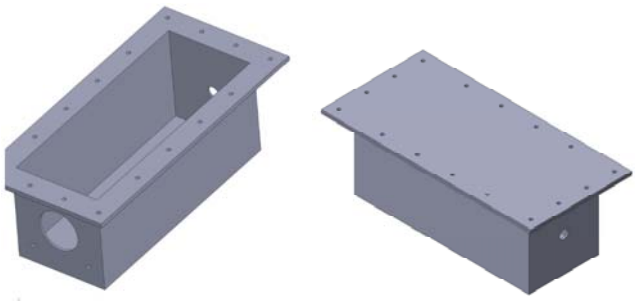

*Figure 2-12 The graphical design of the new heat exchanger outer casing*

The heat exchanger was fabricated at KFUPM workshop and it consists of 4 main parts, which are the shell, the cover, the internal tube and the water coil. Figures 2.13 to 2.16 show all parts of

the new heat exchanger. The number and diameter of holes in the internal pipe was designed in oreder to achieve the required heat transfer and at the same time do not cause back pressure on the engine.

*Figure 2-13 The internal pipe with holes*

*Figure 2-14 The feed water heating coil*

*Figure 2-15 The box containing the exhaust tube with the coil*

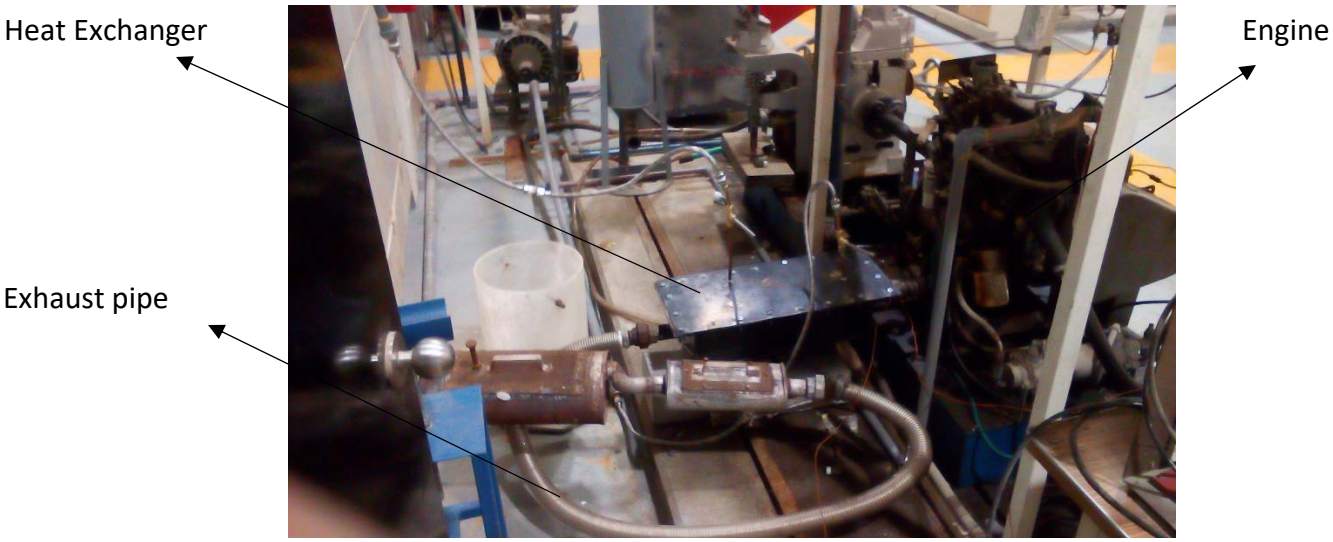


*Figure 2-16 Assembled heat exchanger attached to the engine exhaust line.*

To some extent, the new heat exchanger achieved the required water temperatures and flow rates. Figures 2.17 and 2.18 show some results that were obtained using the new heat exchanger.

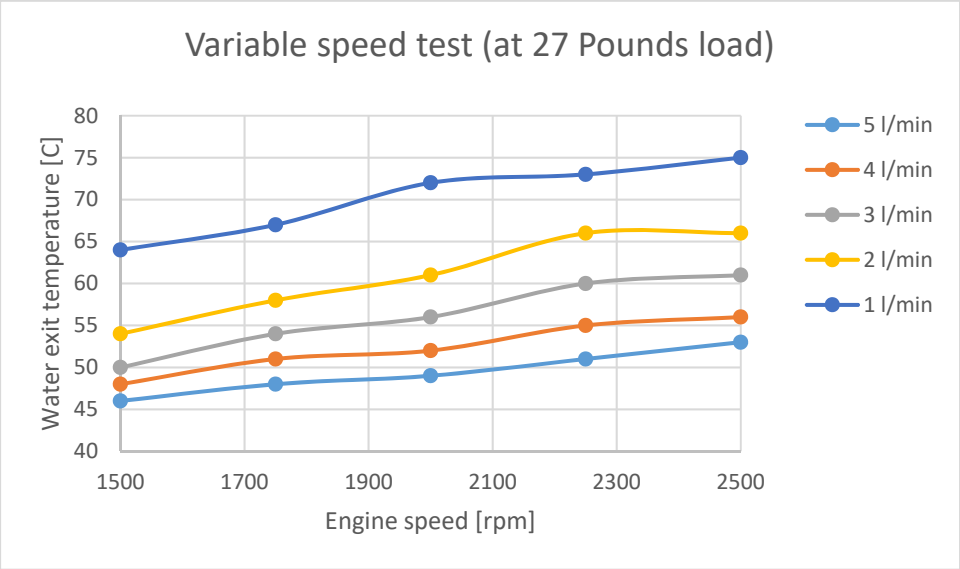


*Figure 2-17 Constant speed test at 2200 rpm showing the change in water temperature with engine speed at different water flow rates for an open water cycle.*

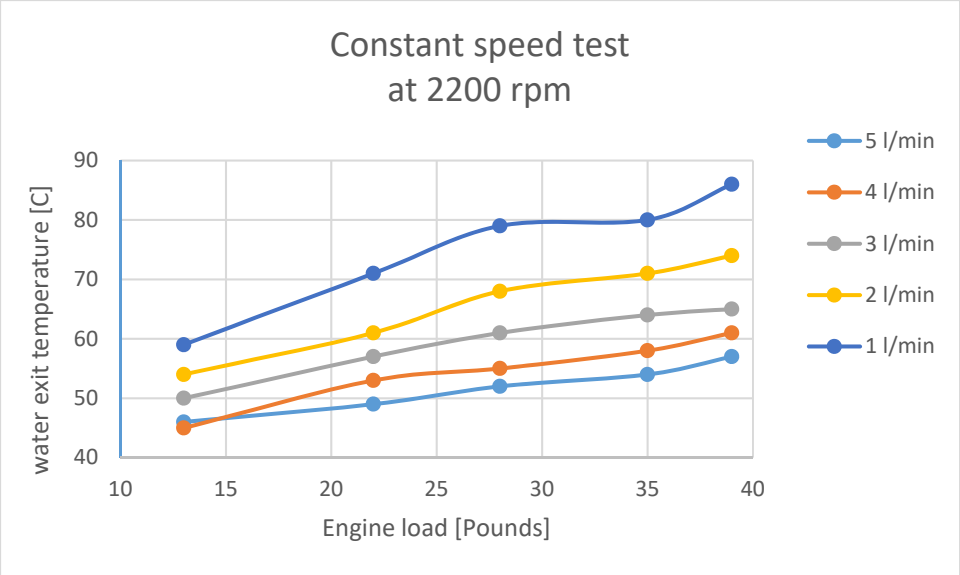


*Figure 2-18 Variable speed test showing the change of water temperature with Engine load at different water flow rates for an open water cycle.*

**Effect of insulation**

Figures 2.20 to 2.23 show the effect of insulating the heat exchanger shown in figure 2.19. Experiments were carried out at 4 different speeds with constant load to show the effect of insulating the heat exchanger on water exit temperature. The exit water temperature is higher in case of insulated heat exchanger at all speeds and different flow rates. It is also noted that the effect of insulation is higher at lower flow rates.

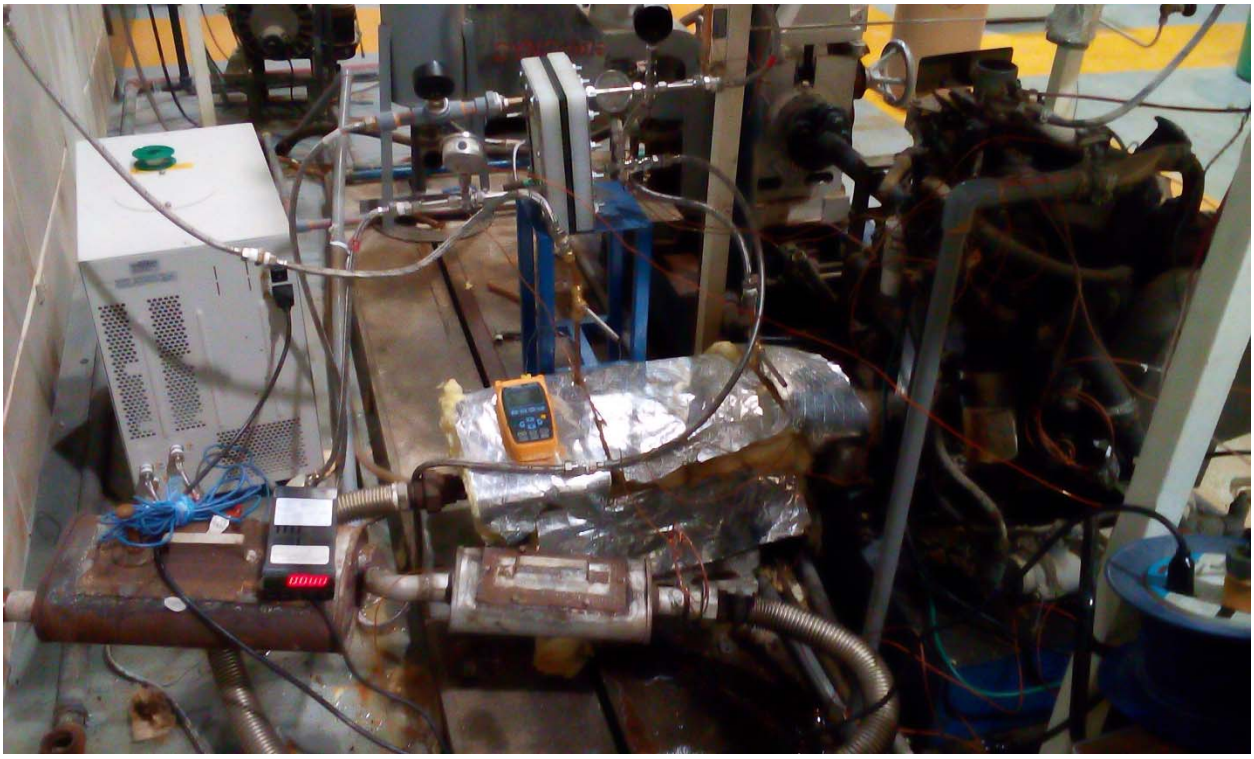

*Figure 2-19 insulated heat exchanger.*

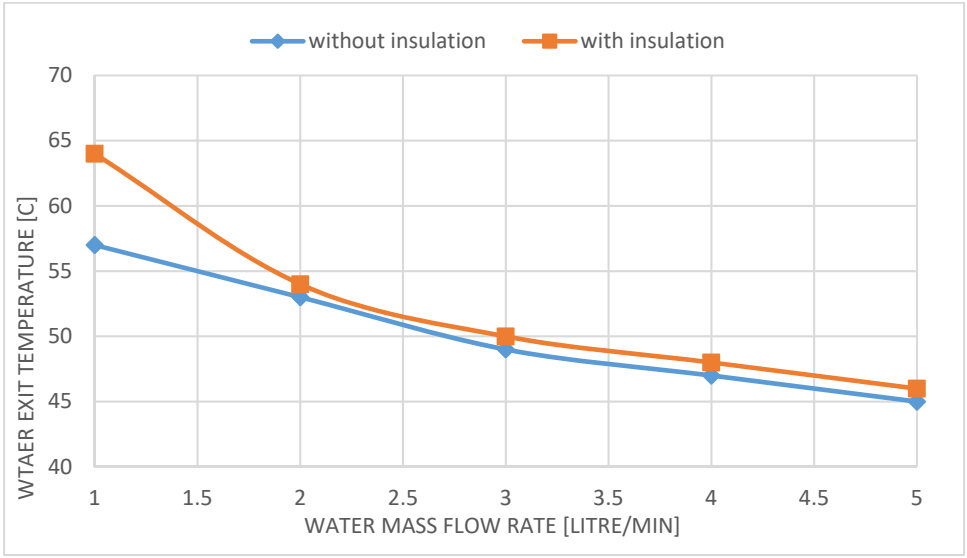


*Figure 2-20 Effect of heat exchanger insulation at 1500 rpm, load of 27 pounds and different flow rates.*

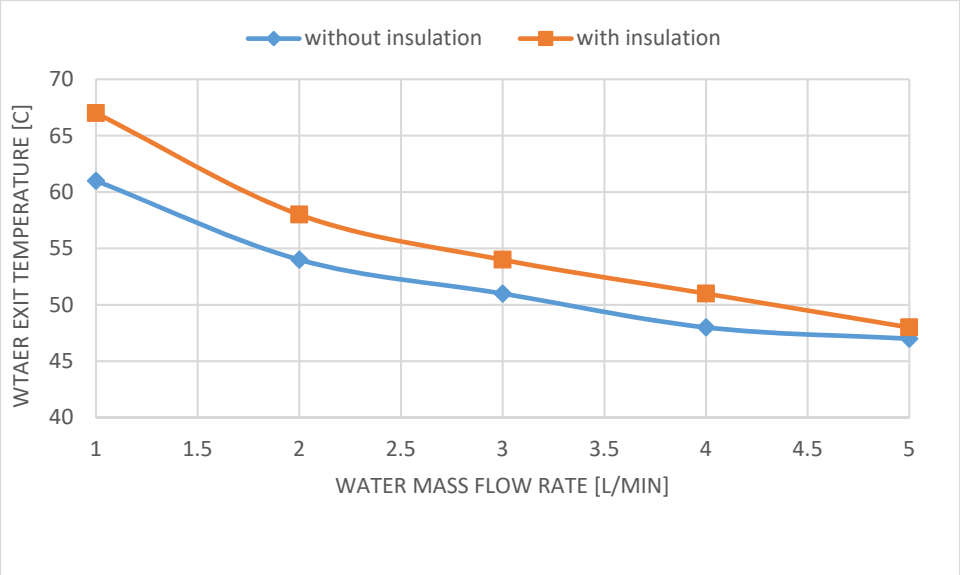


*Figure 2-21 effect of heat exchanger insulation at 1750 rpm, load of 27 pounds and different flow rates.*

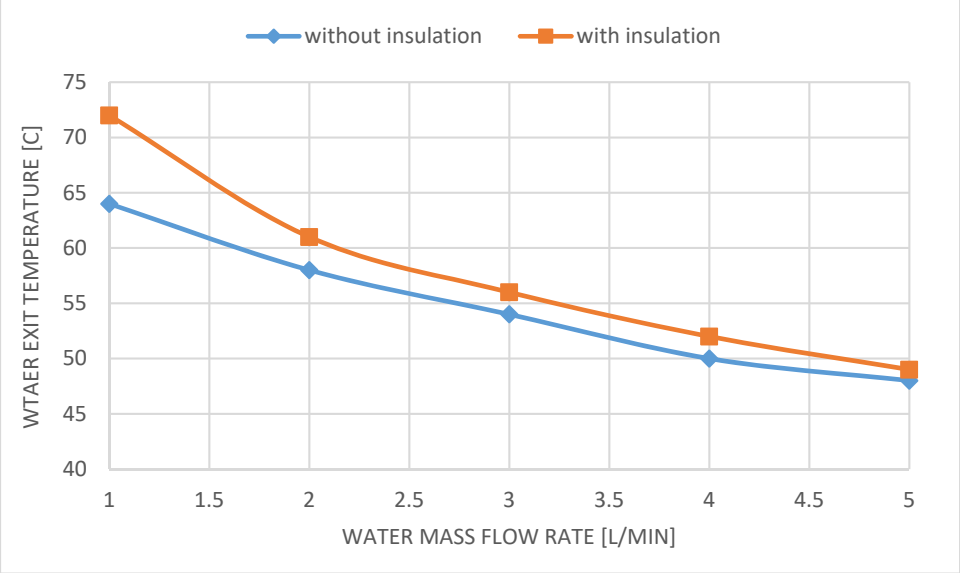


*Figure 2-22 effect of heat exchanger insulation at 2000 rpm, load of 27 pounds and different flow rates.*

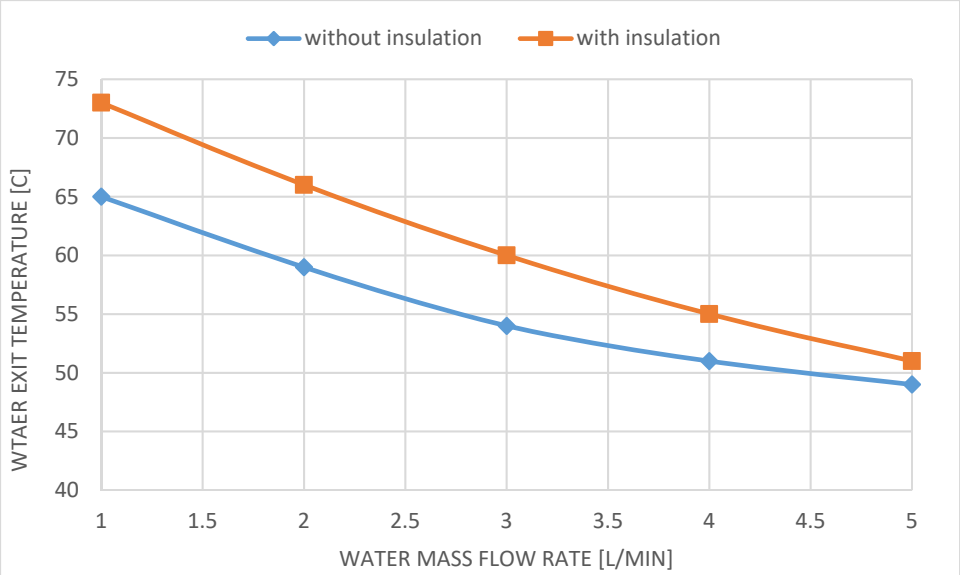


*Figure 2-23 effect of heat exchanger insulation at 2250 rpm, load of 27 pounds and different flow rates.*

**2.4 Conclusion**

A heat exchanger was designed to achieve maximum heat transfer between feed water and the engine exhaust. A theoretical design was carried out using Effectiveness-NTU method. Parametric studies were carried out to show the effect of different variables on tube coil length and water exit temperature from heat exchanger. We started with fabricating a heat exchanger that didn't fulfil our water flow rate requirement due to the small size of water coil. We did some modifications to the fabricated heat exchanger, but it didn't achieve the required water temperature, although it allowed higher water flow rates. Finally, we designed a new heat exchanger and fabricated it in ME/KFUPM workshop. The new heat exchanger fulfilled our requirement of higher flow rates, and to some extent, it achieved higher water temperatures.

# Chapter 3: Experimental results and discussion

## 3.1 Introduction

The scope of this chapter is to present the main part of experimental work done for this thesis, while the other experimental work is presented in the heat exchanger chapter. The purpose of doing these experiments was to test the feasibility of using car engine exhaust to heat a membrane distillation module feed water to provide an access for potable water in areas that have pure water scarcity. This system not only provide a cheap source of energy for water desalination, but also provide a portable water desalination that can be attached to any vehicle. Also, the effect of different variables on system main parameters was assessed through these experiments. After going through many design phases for the heat exchanger, we were able finally to achieve the design that fulfill our flow rate and temperature needs as explained in detail in heat exchanger chapter. At the end, the system showed an ability to achieve the purpose of these experiments as will be explained in this chapter.

## 3.2 Experimental setup

The following two figures represent the real experimental setup. Water from water tank is pumped through CPVC pipe to enter the well-insulated heat exchanger where it gains heat from the exhaust gases coming from engine manifold through exhaust pipe. Hot water leaving the heat exchanger then enters air gap membrane distillation module, where part of it passes through the membrane as a distillate, and the other part is brought back to the water tank causing the water temperature in the tank to increase.


*Figure 3-1 Real photo of the experimental setup.*

The four-cylinder gasoline engine in figure 3.2 is equipped with speed and load controllers and meters to control and monitor engine load and speed during experiments. The dynamometer attached to the engine is used to control engine's load. The exhaust pipe of the engine is well insulated to maintain the heat contained in exhaust gases as possible.

*Figure 3-2 Engine and dynamometer used in experiments.*

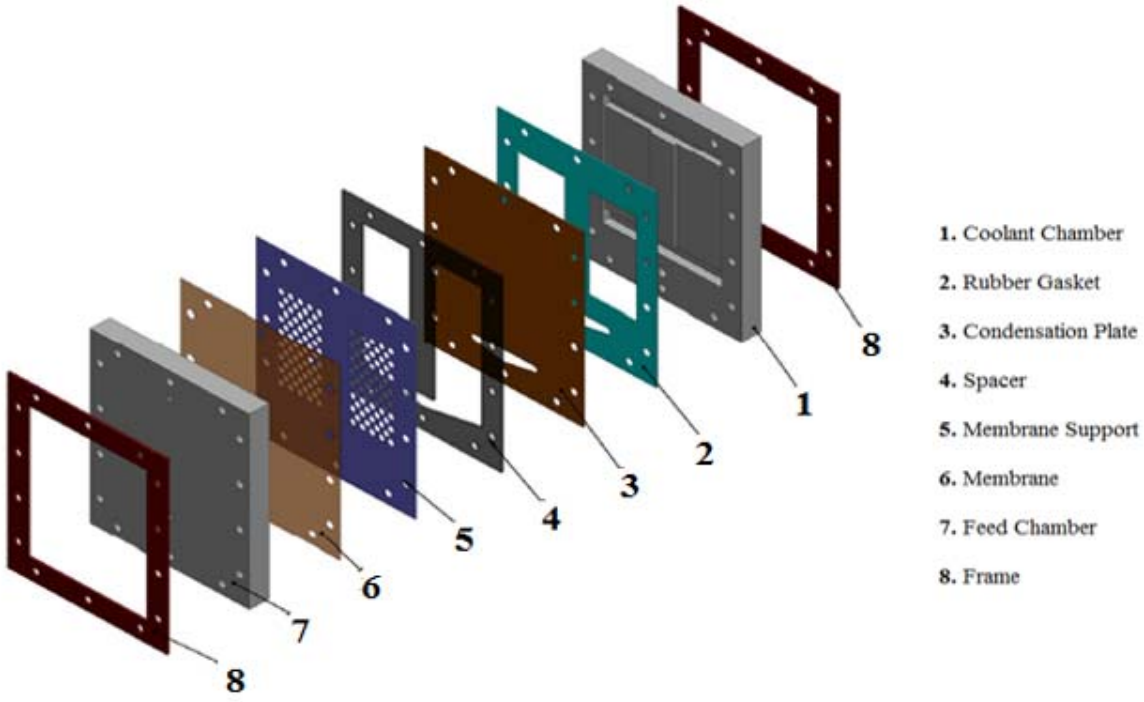


*Figure 3-3 an exploded view of the AGMD used in the experimental setup*

**Experimental procedure**

The basic experimental plan included 27 experiments as a matrix of 3 speeds, 3 loads and 3 flow rates, in addition to other experiments. Every experiment was done at specific load, speed and flow rate, to assess the effect of these variables on main parameters. All experiments were carried out with 4 liter/min cooling water flow rate at a temperature of 32 °C.

Following steps were taken each experiment:

- plug electricity
- make sure fuel tank has enough fuel for the whole run

- Open water main valve
- adjust tank water level at 20 liters and keep it closed
- adjust coolant flow rate at 4 liter/min
- open pump
- adjust feed water flow rate.
- open engine cooling water
- make sure engine is on low load and speed before running
- run the engine
- adjust engine speed and load
- start taking temperature readings using the thermometer
- measure distillate flux using a stop watch and a scaled cup
- keep checking and adjusting flow and speed
- measure salinity using salinity meter
- reduce load and speed
- turn off the engine
- close the main water valve, engine water, pump, coolant valve and unplug electricity

### 3.3 Results

This section presents the results obtained from the experiments carried out. The following four figures represent the results of one experiment. Figure 3.4 shows the variation of inlet and exit

exhaust temperatures with time. The inlet exhaust seems to increase until it reaches a steady state temperature, while the exit exhaust temperature keeps increasing but slowly. Figure 3.5 indicates that both water inlet and exit temperatures keep increasing with time until the exit temperature reaches 90 °C the engine is turned off so as not to exceed the previously set maximum temperature of 90 °C. Figure 3.6 shows the increase of distillate flux with time as the feed water temperature is increasing as the pressure difference across the membrane which is the cause of distillate flux is thermally driven by the temperature difference between feed water and cooling water. Figure 3.7 shows that the salinity is decreasing as the feed water temperature increase with time.

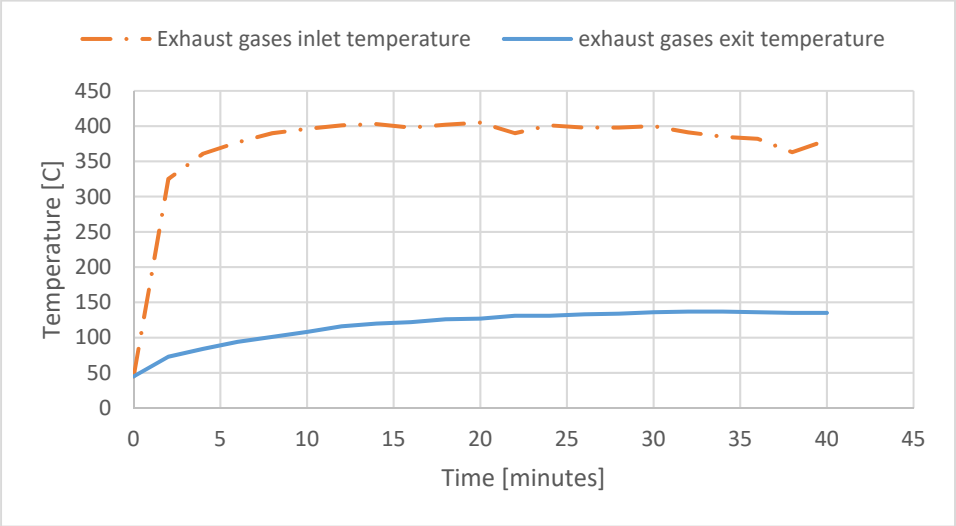


*Figure 3-4 Heat exchanger exhaust gases inlet and exit temperatures variation with time at 2000 rpm, 30 N.m load and 5 LPM feed flow rate.*

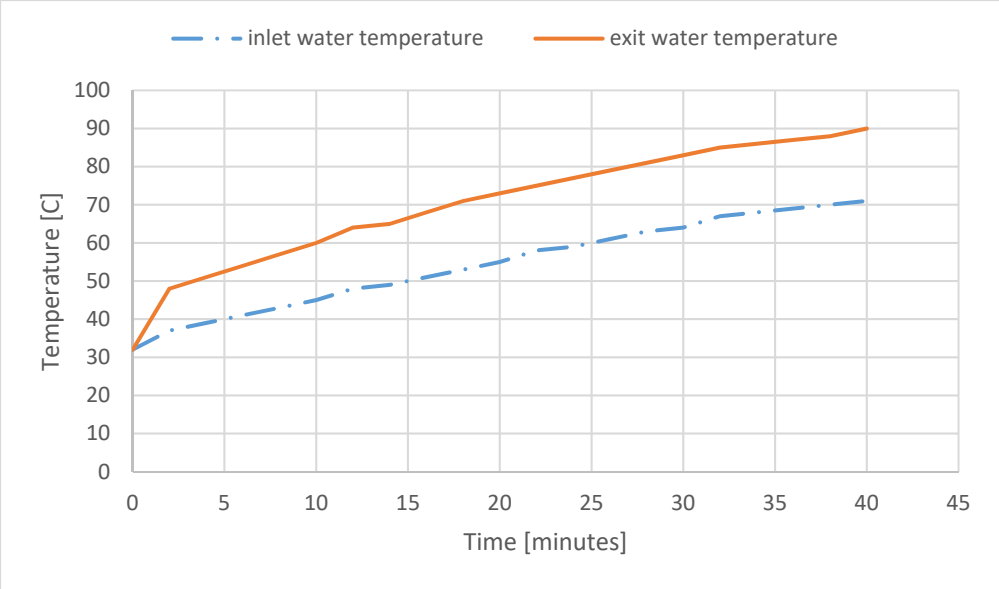


*Figure 3-5 Heat exchanger inlet and exit water temperatures variation with time at 2000 rpm, 30 N.m load and 5 lpm feed flow rate.*

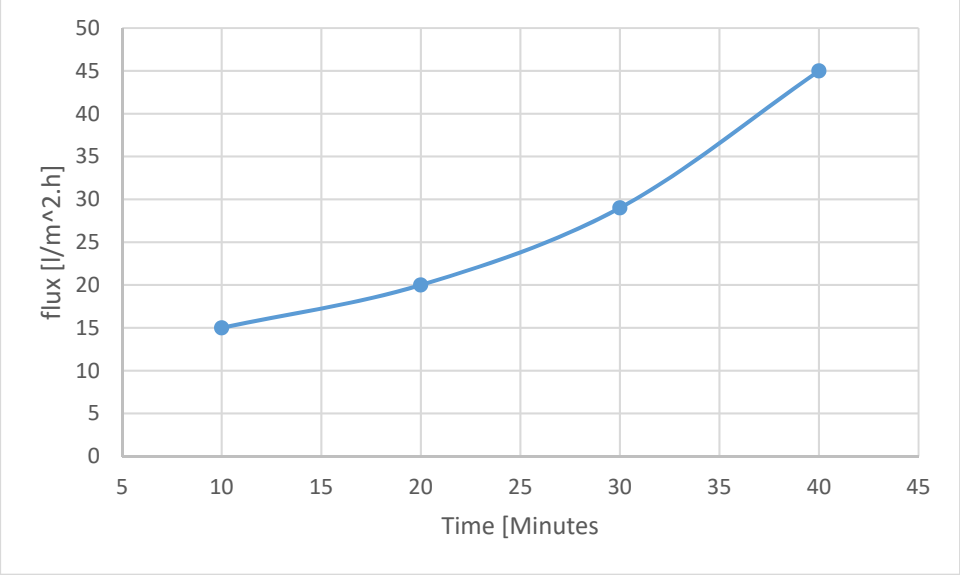


*Figure 3-6 Distillate Flux variation with time at 2000 rpm, 30 N.m load and 5 lpm feed flow rate.*

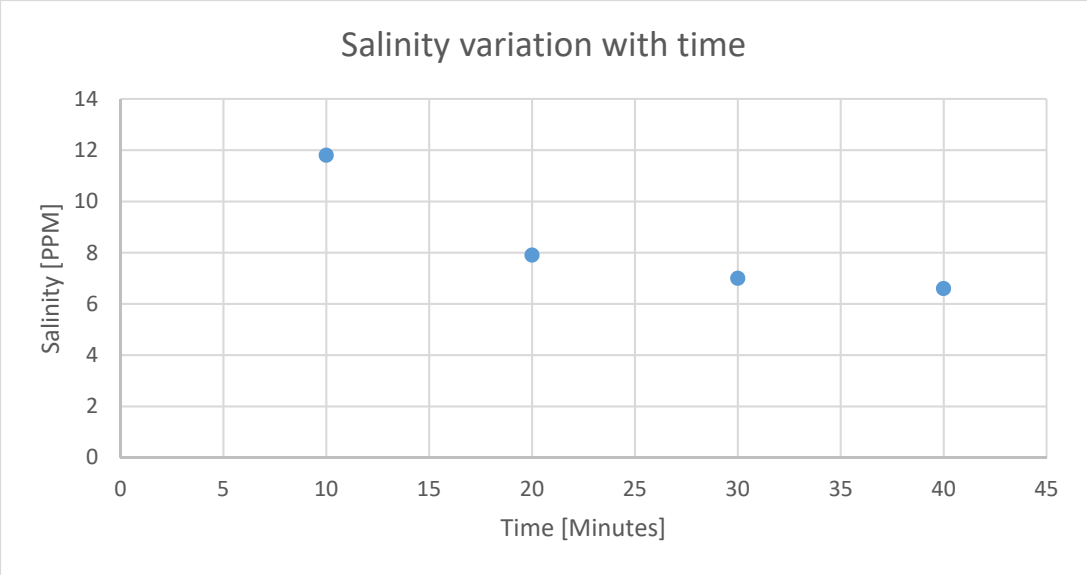


*Figure 3-7 Salinity variation with time at 2000 rpm, 30 N.m load and 5 lpm feed flow rate.*

**Effect of different variables on water exit temperature**

Figure 3.8 shows the effect of load variation on water exit temperature from the heat exchanger. As the load increases, the exit temperature of the heat exchanger also increases due to the higher amount of heat that the water gains from exhaust. And for the same reason the temperature of water increases as the speed of the engine is increased as shown in figure 3.9 as the power of the engine increases releasing higher energy in the exhaust. While increasing the water flow rate caused the exit water temperature to decrease as shown in figure 3.10 as now the same amount of heat is given to higher amount of water. It was noted that increasing the load is more effective than increasing the speed. We can also note the time variation between the three cases to reach the previously set maximum feed water temperature of 90 °C. for 30 N.m load, it takes only 8

minutes to reach the maximum temperature, while it takes 12 minutes for 42 N.m load and 16 minutes for 52 N.m load.

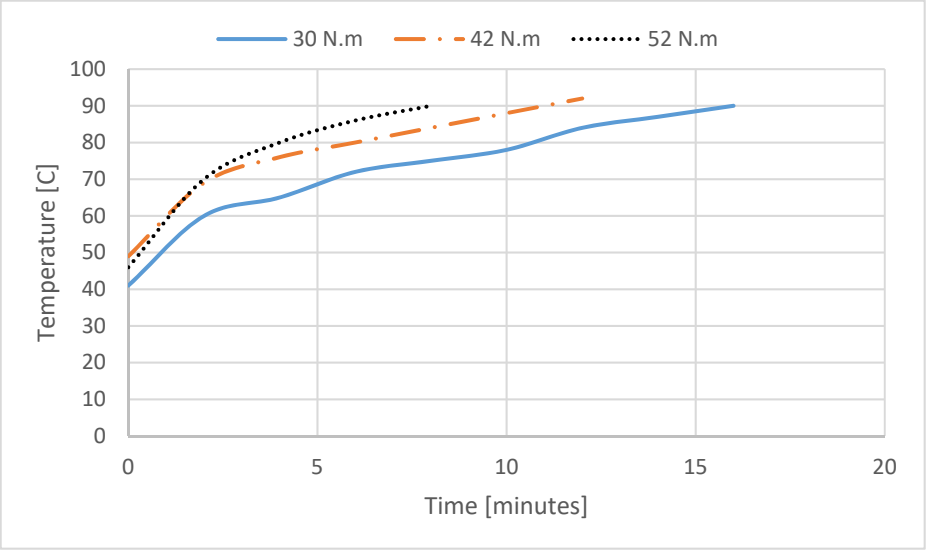


*Figure 3-8 Effect of variation of engine load on feed water exit temperature from heat exchanger at 2800 rpm and 3 l/min feed water flow rate*

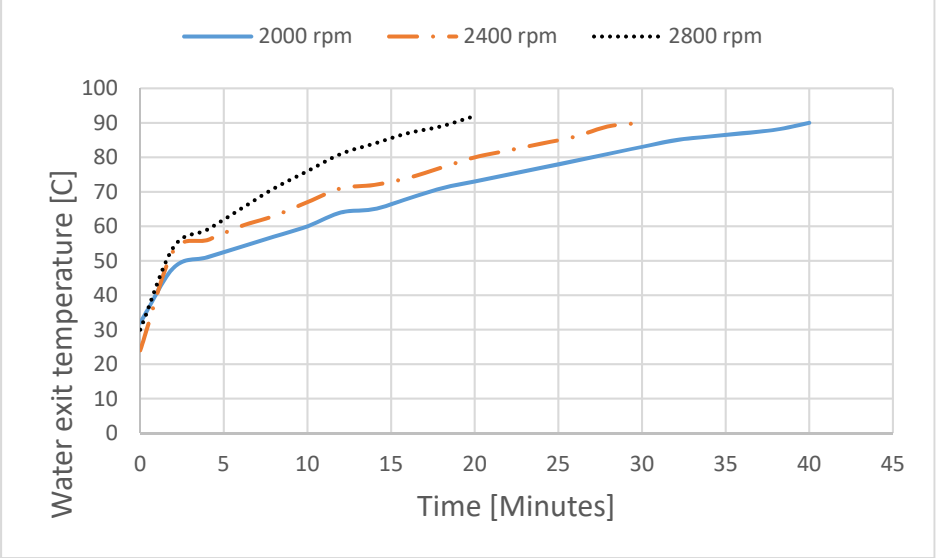


*Figure 3-9 Effect of variation of engine speed on water exit temperature from heat exchanger at 30 N.m load and 5 l/min feed flow rate*

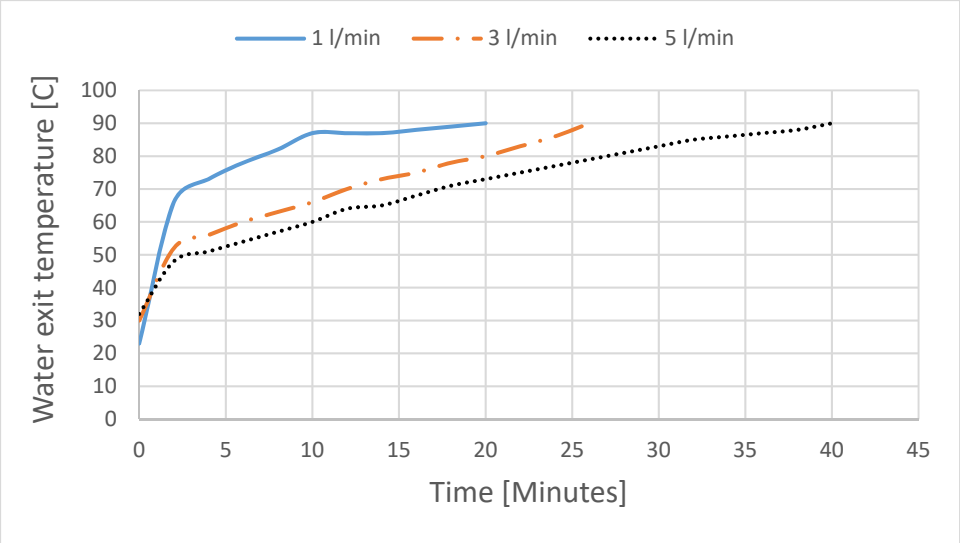


*Figure 3-10 Effect of variation of feed water flow rate on feed water exit temperature from heat exchanger at 2000 rpm & 30 N.m*

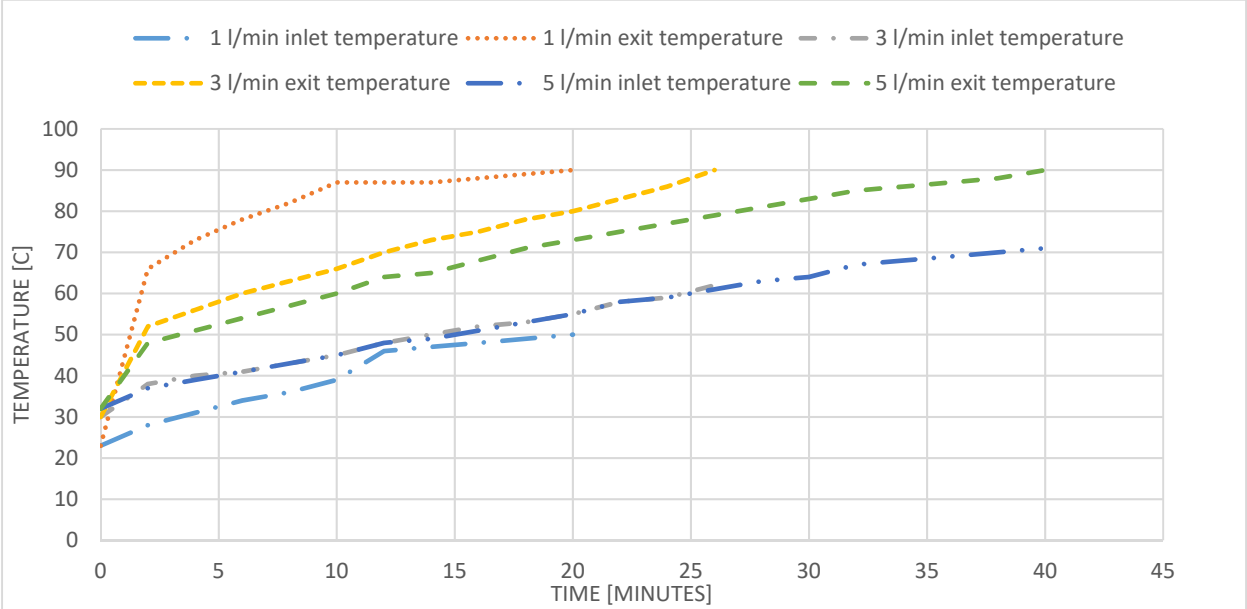


*Figure 3-11 Effect of variation of feed water flow rate on feed water temperature difference at 2000 rpm and 30 N.m load*

It was noted that increasing the feed water flow rate cause a decrease in temperature difference between feed water inlet and exit temperatures. Figure 3.11 clarifies that effect.

To assess the effect of opening the feed water tank to atmosphere, the same experiment was done twice, one time with tank open and the second with tank closed. The aim of opening the tank is to clarify the effect of heat convection between hot feed water in the tank and the atmospheric air, which will affect the MD performance. Figure 3.12 shows the temperature difference between the two cases at a certain time. It also shows the difference in time needed in each case to reach 90 °C.

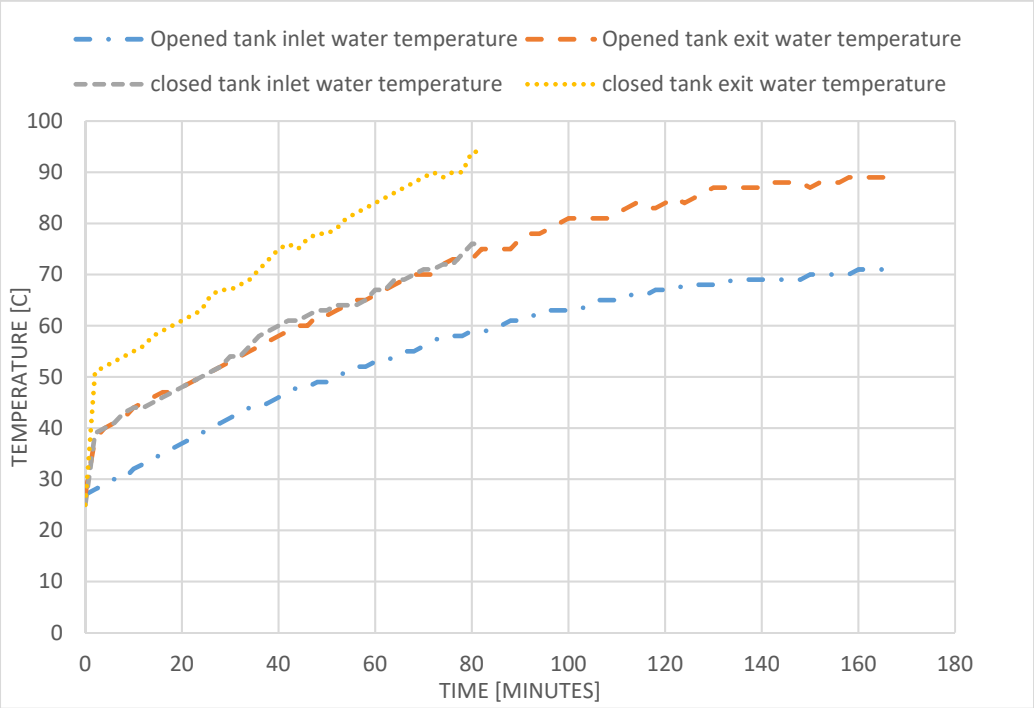


*Figure 3-12 Inlet and exit feed water temperatures variation with time for opened and closed tank*

**Effect of different variables on distillate flux**

The following three figures show the effect of engine load, engine speed and feed water flow rate on the distillate flux. Figure3.13 and 3.14 indicate that the flux increases with increasing the load and speed, as increasing the load or speed causes an increase in feed water temperature as seen before. We can see that the time limit varies for each load, since the time needed to reach 90 °C decreases as the load decreases. Figure 3.15 shows that increasing the feed water flow rate leads to a decrease in flux, as increasing the flow rate leads to a decrease in feed water temperature. But when feed water reaches a steady state temperature, increasing its flow rate will lead to an increase in distillate flux. Figure 3.16 shows the effect of opening the tank to atmosphere on distillate flux. The distillate flux is higher in case of closed tank because of higher feed temperatures.

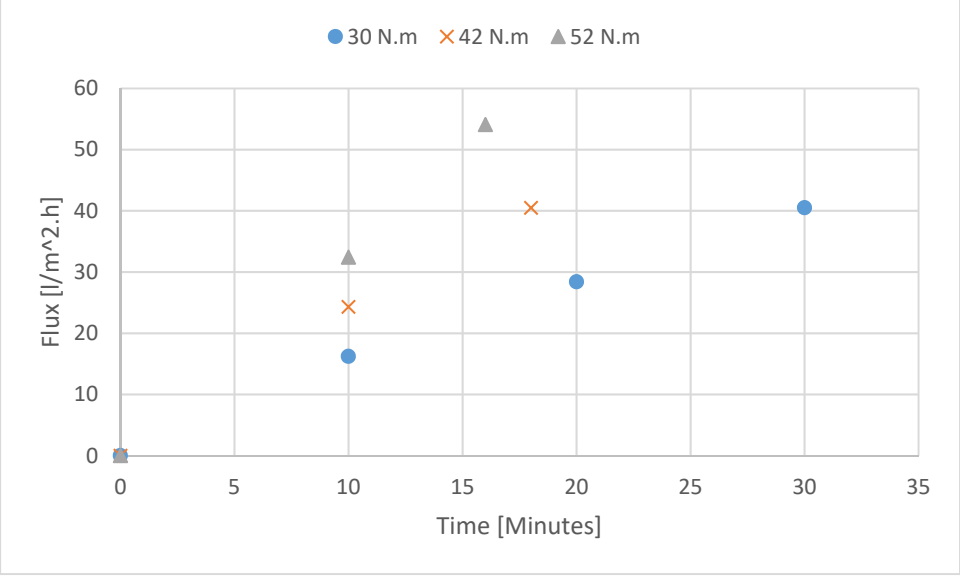


*Figure 3-13 Effect of engine load variation on Distillate flux at 2400 rpm and 5 l/min feed flow*

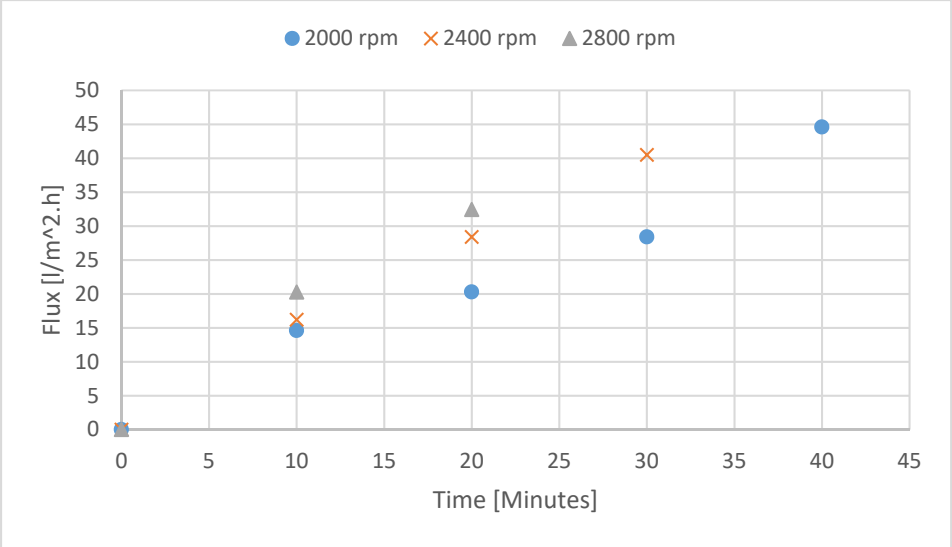


*Figure 3-14 Effect of engine speed variation on distillate flux at 30 N.m load and 5 l/min feed flow rate*

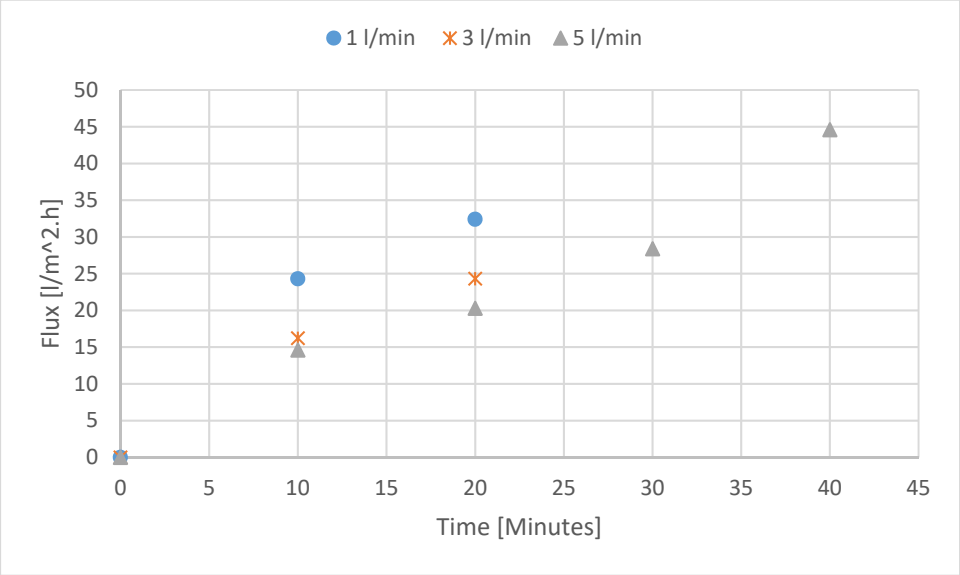


*Figure 3-15 Effect of feed water flow rate variation on distillate flux at 2000 rpm and 30 N.m load*

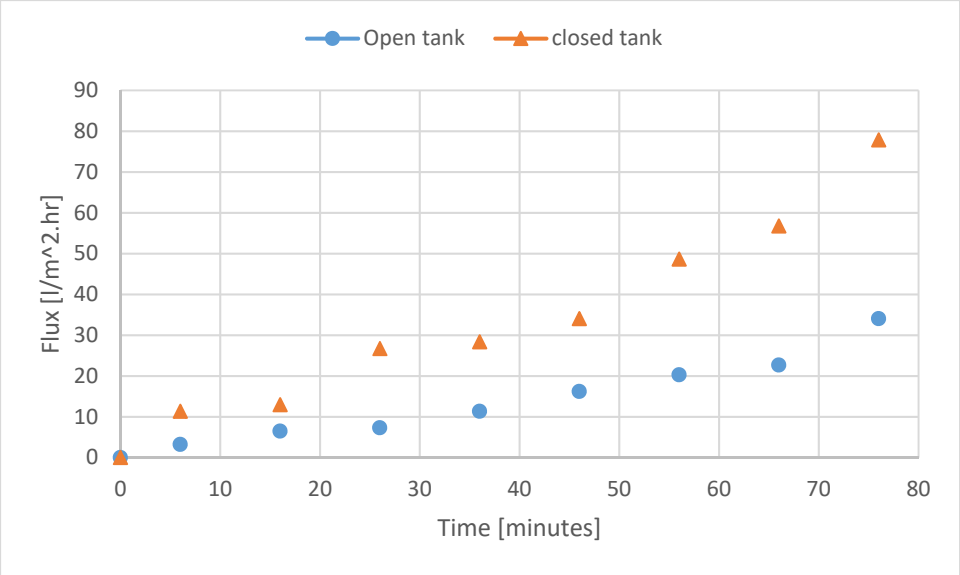


*Figure 3-16 Variation of distillate flux with time for opened and closed tank at 2000 rpm, 30 N.m load and 5 LPM feed flow rate.*

**Different variables effect on exhaust inlet temperature**

As the load or speed of the engine increases, the exhaust temperature increases due to higher energy generated in the engine exhaust at higher engine powers, as shown in figure 3.17 and 3.18.

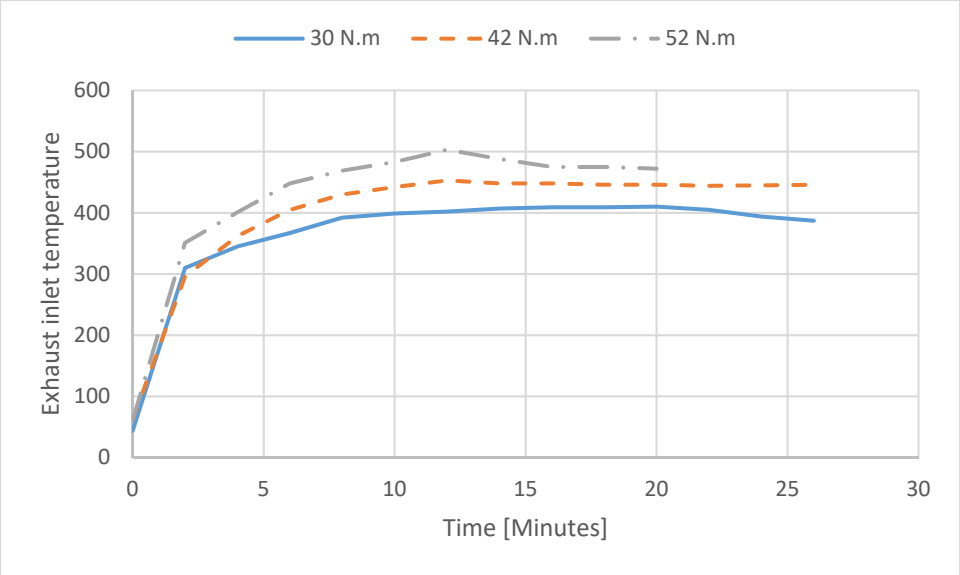


*Figure 3-17 Effect of load variation on exhaust inlet temperature at 2000 rpm*

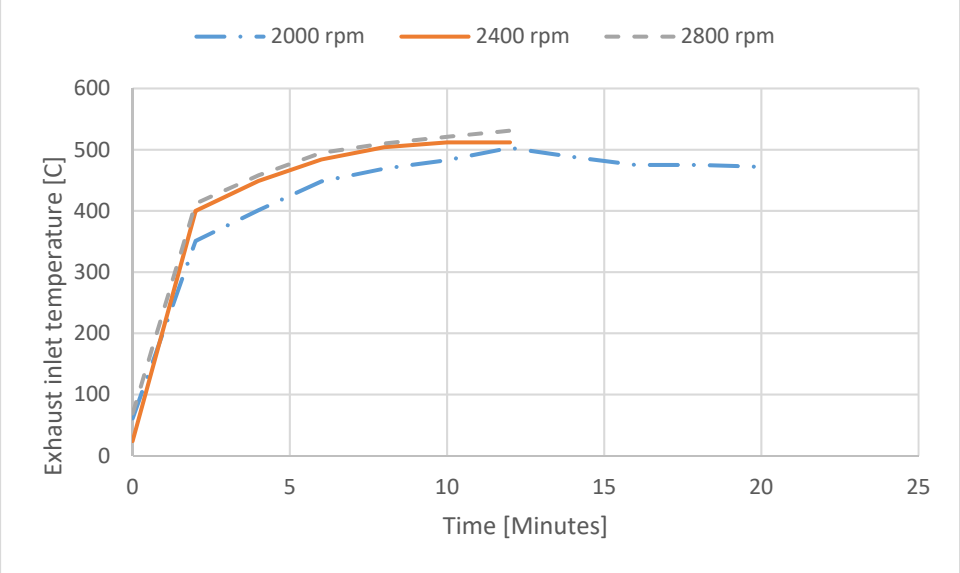


*Figure 3-18 Effect of speed variation on exhaust inlet temperature at 35 pounds*

**Specific fuel consumption**

The following two figures shows the specific fuel consumption variation for both constant speed and constant load experiments. The importance of these figures is to show where are the points where the BSFC is high and where it is lower, and to find out the average specific fuel consumption of the system.

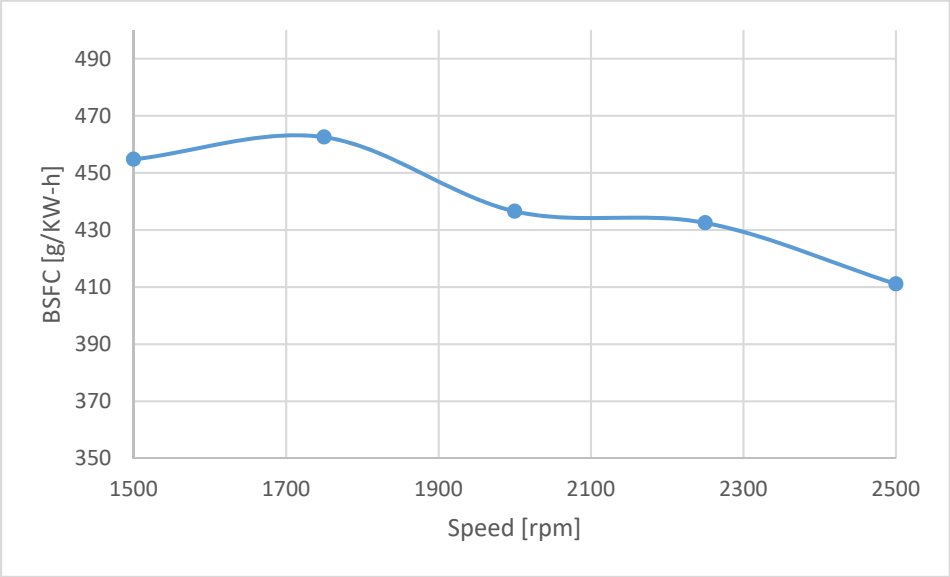


*Figure 3-19 Specific fuel consumption variation with speed at 42 N.m Pounds load*

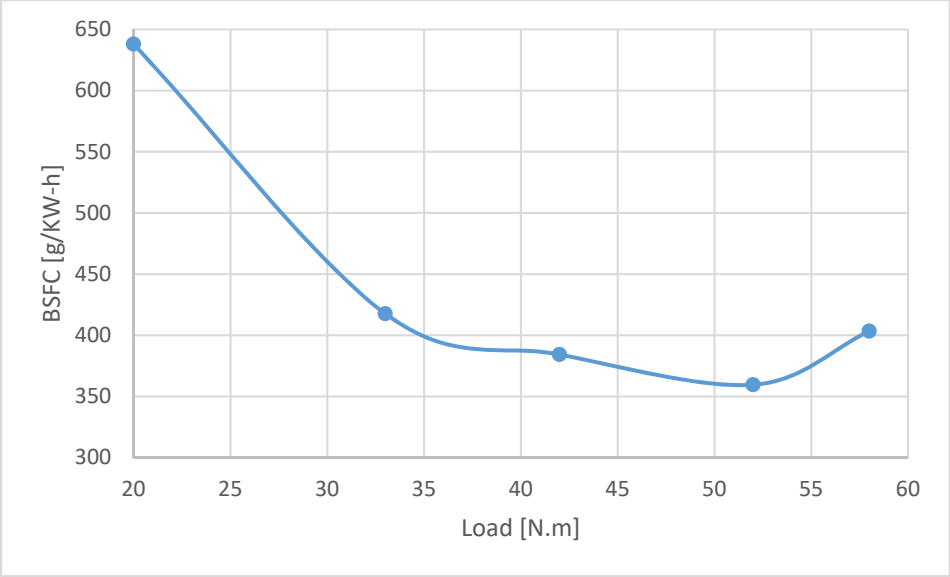


*Figure 3-20 Specific fuel consumption variation with load at 2200 rpm*

**3.4 Conclusion**

A list of experiments was carried out to assess the feasibility of heating the feed water of a MD module by car engine exhaust gases through a heat exchanger. The effect of different variables on main parameters was observed through comparative figures. The system shows a good capability of achieving its mission. The distillate flux was found to increase with increasing engine load and speed, however, increasing engine load had more significant effect on distillate flux than increasing engine speed. Distillate flux was found to decrease with increasing feed water flow rate at the same engine load and speed. Also, distillate flux was increasing faster when the feed water tank was closed compared to open feed water tank. The average specific fuel consumption of the engine was about 425 g/KW-h.

# Chapter 4: Exergy analysis

## 4.1. introduction

The property exergy [35] to [41] is defined as the potential of a system to do work in its environment, or, in other words, it is the maximum amount of work which can be obtained if the system is brought into equilibrium with its environment. Unlike energy, exergy is not conserved (except for ideal processes), it is destroyed due to irreversibilities in any real processes.

The following figure explains the difference between the concept of exergy and energy. Where unavailable energy is the energy which can't be transferred into useful work.

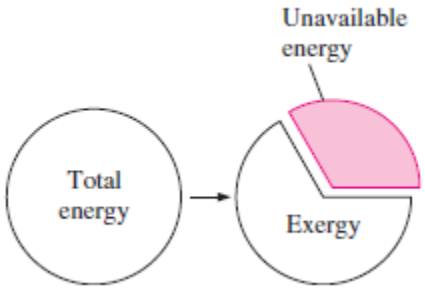


*Figure 4-1 Difference between exergy and energy.*

Exergy analysis is carried out to know which parts of any systems are responsible for most of exergy destructions, so, it is an efficient tool for improvement and understanding of processes.

Banat et al. [42] used exergy analysis for the evaluation of exergy efficiency of the solar powered membrane distillation unit in figure 6.

Exergy is the maximum amount of work which can be obtained as a certain system is brought into equilibrium with its environment. Exergy, unlike energy, is not conserved (except for ideal or reversible processes). Because of irreversibilities in all real processes, exergy is consumed or destroyed. The following equation is the general form of exergy balance for any system or process:

$$\begin{pmatrix}\text{Total}\\ \text{exergy}\\ \text{entering}\end{pmatrix}-\begin{pmatrix}\text{Total}\\ \text{exergy}\\ \text{leaving}\end{pmatrix}-\begin{pmatrix}\text{Total}\\ \text{exergy}\\ \text{destroyed}\end{pmatrix}=\begin{pmatrix}\text{Change in the}\\ \text{total exergy}\\ \text{of the system}\end{pmatrix}$$

Applying Exergy analysis identifies the system's components, which can be further improved. When exergy destroyed is high in a certain part, then, this part should be improved. The following equation describes the exergy of a substance at any point.

$$Ex = \dot{m}\psi = \dot{m}\left[ h - h_0 - T_0 \left( s - s_0 \right) \right]$$

It was found that among the system components, the separation process in the MD brings the most exergetic losses; it accounts for 55.14% of the total input exergy. The exergetic losses in the heat exchanger accounts for 42.73% of the total exergy input. Increasing the surface area of the membrane is a reasonable practice to increase the efficiency. Increasing the membrane surface area is an option to increase energy recovery and hence, decreasing exergy destruction, but its cost effectiveness must be considered. The exergy efficiency of the compact system in figure 6 is 0.01%. The increase of solar insolation was associated with an increase of collector exergy efficiency.

**4.2. Exergy analysis**

We will be assuming the following in this exergy analysis:

1) The kinetic and potential energies of fluid streams are negligible.
2) Adiabatic heat exchanger.

The following equation represents a balance of exergy for any system and process:

(Total exergy entering) - (Total exergy leaving) - (Exergy destroyed) = (Change of total exergy of the system)

Where, exergy at a point relative to the environment is obtained from

$$Ex = m(h - h_0 - T_0(s - s_0))$$

Where,

Ex, is the exergy at this point

m is the mass

h & $h_0$ are the enthalpies at this point and at environment conditions respectively

s & $s_0$ are the entropies at the specified point and environment conditions respectively

$T_0$ is the environment temperature

Figure 4.2 is a simplified a lay out of the system. The exhaust gases coming from the engine passes through the heat exchanger heating the feed water entering MD module. Part of feed water passes through the membrane while the rest comes out of the MD module as a brine. Cooling water passes through the MD module to achieve the necessary temperature difference that is the root cause of pressure difference motivating water mass transfer.

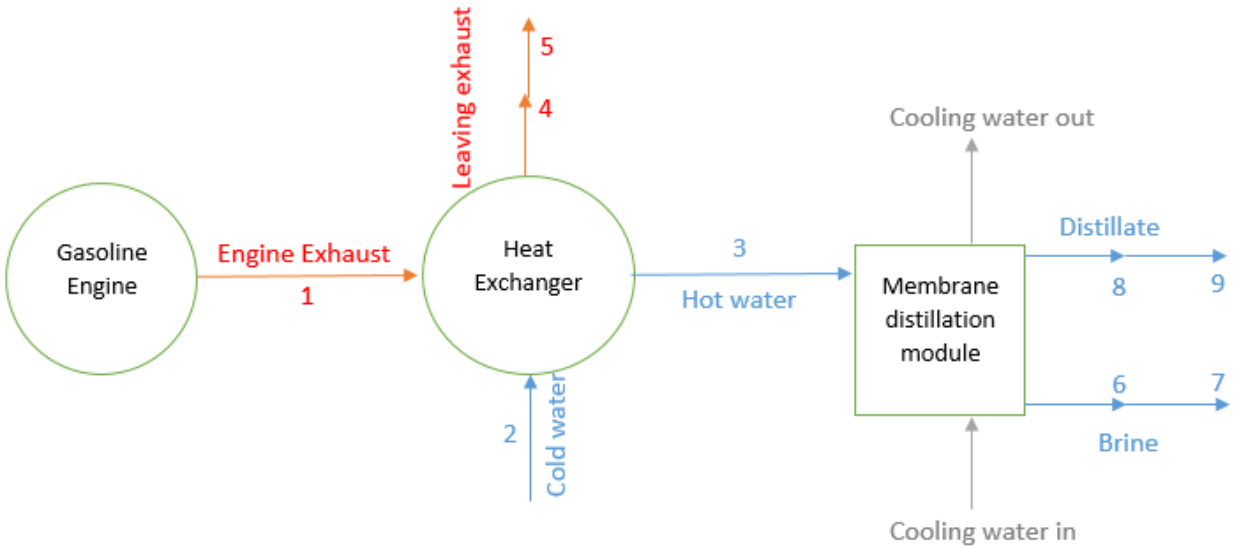


*Figure 4-2 Simplified open cycle system layout for exergy analysis*

### 4.2.1 Calculation of water and exhaust outlet temperatures from heat exchanger

From heat balance, and given water and exhaust inlet temperatures

$$m_{exhaust} * Cp_{exhaust} * (T_{exhaust\ in} - T_{exhaust\ out}) = m_{water} * Cp_{water} * (T_{water\ out} - T_{water\ in})$$

Then the Effectiveness-NTU method is used to have two equations in two unknowns.

Water heat capacity is $C_{water} = m_{water} * Cp_{water}$

& exhaust heat capacity is $C_{exhaust} = m_{exhaust} * Cp_{exhaust}$

Then after knowing which heat capacity is the smaller and which is the maximum we calculate the heat capacity ratio as

$$C_r = \frac{C_{min}}{C_{max}}$$

And then the number of transfer units is found from

$$NTU = U * \frac{A_h}{C_{min}}$$

Where $A_h$is the heat transfer area, and $U$ is the overall heat transfer coefficient which is calculated in detail in heat exchanger chapter. Then using NTU and $C_r$ the effectiveness ϵ is determined from charts.

Also $q_{max} = C_{min} * (T_{exhaust\ in} - T_{water\ in})$

And the heat transferred is $q = \epsilon * q_{max}$

Finally, the heat transfer is also $q = m_{exhaust} * Cp_{exhaust} * (T_{exhaust\ in} - T_{exhaust\ out})$

### 4.2.2 Calculations of entropy and enthalpy at a point for saline water

Calculation of entropy and enthalpy will follow that saline water can be considered as a mixture of water and salt.

#### 4.2.2.1 Enthalpy calculation

For calculating enthalpy at a point, we will use the following equation:

$$h_{mixture} = w_{salt} * h_{salt} + w_{water} * h_{water}$$

Where,

$h_{mixture}$ : is the enthalpy of the mixture.

$h_{salt}$ & $h_{water}$ : are the enthalpy of salt and water respectively as a pure substance at this point.

$w_{salt}$ & $w_{water}$ : are the weight fractions of salt and water respectively

And,

$$h_{salt} = Cp_{salt} * T(in\ K)$$

And water enthalpy is obtained from tables at the point's pressure and temperature.

#### 4.2.2.2 Entropy calculation

The entropy of a component in a mixture is always greater than the entropy of that component when it existed alone at the mixture temperature and pressure. So, we can't just calculate the entropy by the same way we used for enthalpy calculation. Rather, the following equation will be used to calculate entropy of the salt and water mixture at a point:

$$s_{mixture} = w_{salt} * s_{salt_{pure}} + w_{water} * s_{water_{pure}} - R_{water} * (x_{salt} * \ln(x_{salt}) + x_{water} * \ln(x_{water}))$$

Where,

$s_{salt_{pure}}$ & $s_{water_{pure}}$ : are entropies of salt and water as pure substances, respectively

$R_{water}$ = 461.5 [j/kg*k]

$x_{salt}$ & $x_{water}$ : are mole fractions of salt and water, respectively

And,

$$s_{salt_{pure}} = s_{salt_{standard}} + Cp_{salt} * \ln(T/T_{standard})$$

Where, $s_{salt_{standard}}$ : is the standard salt entropy and equals 1233.92 [j/kg*k]

And,

$$x_{water} = w_{water} * (\frac{M_{mixture}}{M_{water}})$$

$$x_{salt} = 1 - x_{water}$$

$$M_{mixture} = \frac{1}{\left(\frac{w_{water}}{M_{water}}\right) + \left(\frac{w_{salt}}{M_{salt}}\right)}$$

$M_{salt}$= 58.44 [kg/kmol]

$M_{water}$= 18 [kg/kmol]

Where, $M_{water}$ , $M_{salt}$ & $M_{mixture}$ are molar masses of water, salt and mixture respectively.

**4.2.3 calculation of the exhaust mass flow rate, enthalpies and entropies**

**Exhaust flow rate calculation**

for a 2000cc 4 stroke car engine running at 2000 rpm, the air mass flow rate is found from:

air mass flow rate = air density * displaced volume * volumetric efficiency / (4*60)

displaced volume = 2000 * $10^{-6}$ [$m^3$]

volumetric efficiency = 0.97

assuming an air to fuel ratio of 14:1, then the exhaust gas mass flow rate = 1.07 * air mass flow rate [kg/s]

**Exhaust enthalpies calculation**

For gas at temperature T, the gas is treated as a mixture of octane combustion products, and enthalpy is calculated as follows

$$h_{exhaust} = y_{i_{CO_2}} * h_{CO_2} + y_{i_{N_2}} * h_{N_2} + y_{i_{Water}} * h_{Water}$$

Where, $y_i$ is the mole fraction of each component. And the enthalpy of each component is calculated at temperature T.

**Exhaust entropies calculation**

the calculation of entropies will follow the base of enthalpies calculation. The entropy of the gas mixture at a point is found from

$$s_{exhaut} = \left(\frac{1}{M_{octane}}\right) * (M_{CO_2} * s_{CO_2} - R * \ln(y_{i_{CO_2}}) + M_{N_2} * s_{N_2} - R * \ln(y_{i_{N_2}}) + M_{Water} *$$

$$s_{Water} - R * \ln(y_{i_{Water}}))$$

Where, M is the molar mass of each component and R is the universal gas constant.

### 4.2.4 Second law efficiency calculations

Second law efficiency focuses on irreversibilities that need to be dealt with to improve performance. The second-law efficiency for separation processes can be defined as

$$\eta_{\|} = \left(1 - \frac{Ex_{destroyed}}{Ex_{in}}\right) * 100$$

Where,

$\eta_{\|}$ is the second law efficiency

$Ex_{destroyed}$ is the destroyed exergy in system parts

$Ex_{in}$ is the exergy incoming with the engine exhaust

Exergy input from exhaust to water will be

$$Ex_{in} = m_1{*}(h_1 - h_{0_{exhaust}} - T_0(s_1 - s_{0_{exhaaust}}))$$

Minimum work of separation is

$$W_{min} = Ex_6 + Ex_8 - Ex_0$$

$$W_{min} = m_6\big(h_6 - h_0 - T_0(s_6 - s_0)\big) + m_8(h_8 - h_0 - T_0(s_8 - s_0))$$

Exergy destroyed is

$$Ex_{destroyed} = Ex_{in} - W_{min}$$

### 4.2.5 Percentage Exergy destroyed by each component

**Exergy destroyed by the MD**

$$Ex_{destroyed\ in\ MD\ \%} = (\frac{Ex_{destroyed\ in\ MD}}{Ex_{in}})$$

$$Ex_{destroyed\ in\ MD} = Ex_3 - Ex_6 - Ex_8$$

$$m_3(h_3 - h_0 - T_0(s_3 - s_0)) - m_6(h_6 - h_0 - T_0(s_6 - s_0)) - m_8(h_8 - h_0 - T_0(s_8 - s_0))$$

**Exergy destroyed by the heat exchanger**

$$Ex_{destroyed\ in\ H.Ex\ \%} = (\frac{Ex_{destroyed\ in\ H.Ex}}{Ex_{in}})$$

$$Ex_{destroyed\ in\ H.Ex} = Ex_1 + Ex_2 - Ex_3 + Ex_4$$

$$m_1\left(h_1 - h_{0\_exhaust} - T_0(s_1 - s_{0\_exhaust})\right) + m_2(h_2 - h_0 - T_0(s_2 - s_0)) - m_3(h_3 - h_0 -$$

$$T_0(s_3 - s_0)) + m_4\left(h_4 - h_{0\_exhaust} - T_0(s_4 - s_{0\_exhaust})\right)$$

**Exergy destroyed by brine**

$$Ex_{destroyed\ in\ brine\ \%} = (\frac{Ex_{destroyed\ in\ brine}}{Ex_{in}})$$

$$Ex_{destroyed\ in\ brine} = Ex_6 - Ex_7$$

$$m_6\left(h_6 - h_0 - T_0(s_6 - s_0)\right) - m_7\left(h_7 - h_0 - T_0(s_7 - s_0)\right)$$

**Exergy destroyed by distillate**

$$Ex_{destroyed\ in\ distillate\ \%} = \left(\frac{Ex_{destroyed\ in\ distillate}}{Ex_{in}}\right)$$

$$Ex_{destroyed\ in\ distillate} = Ex_8 - Ex_9$$

$$m_8\left(h_8 - h_0 - T_0(s_8 - s_0)\right) - m_9\left(h_9 - h_0 - T_0(s_9 - s_0)\right)$$

**Exergy destroyed by the leaving exhaust**

$$Ex_{destroyed\ in\ exhaust\ \%} = \left(\frac{Ex_{destroyed\ in\ exhaust}}{Ex_{in}}\right)$$

$$Ex_{destroyed\ in\ exhaust} = Ex_4 - Ex_5$$

$$m_4\left(h_4 - h_{0\_exhaust} - T_0\left(s_4 - s_{0\_exhaust}\right)\right) - m_5\left(h_5 - h_{0\_exhaust} - T_0\left(s_5 - s_{0\_exhaust}\right)\right)$$

### 4.2.6 Parametric studies

Parametric studies that show the effect of exhaust inlet temperature and water flow rate on the second law efficiency and water exit temperature from the heat exchanger were carried out. The following three figures show the relations. Figure 4.3 indicates that second low efficiency increases by increasing exhaust inlet temperature and decreases when the feed

water flow rate increases. Figure 4.4 clarifies the direct proportionality between feed water exit temperature from the heat exchanger and exhaust inlet temperature to the heat exchanger. Figure 4,5 shows that second low efficiency is directly proportional to exit temperature from heat exchanger of feed water.

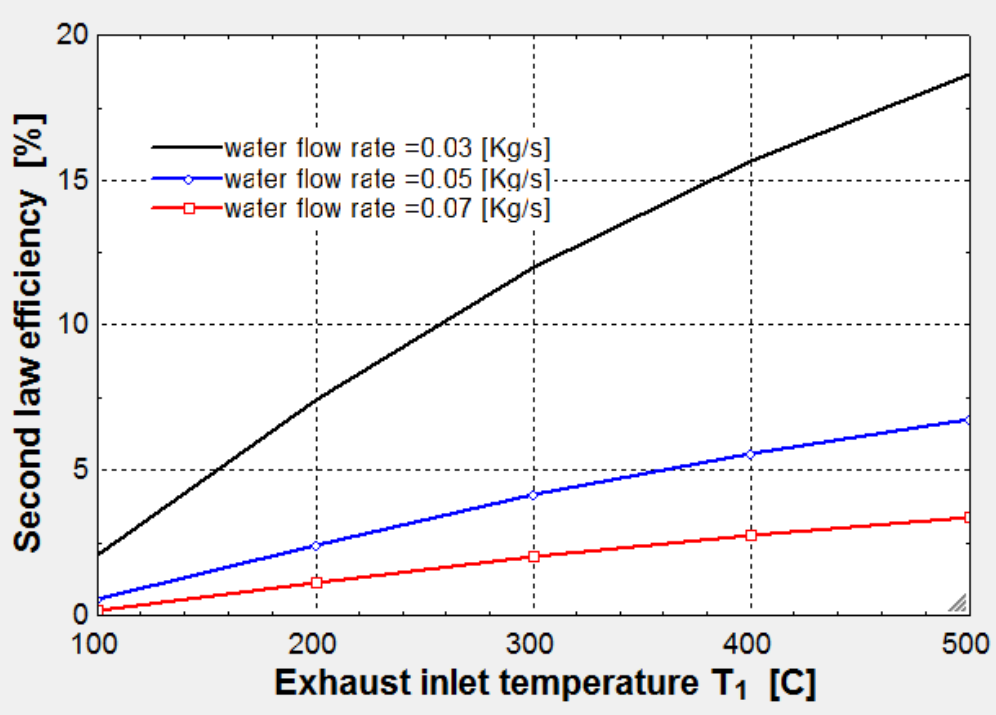


*Figure 4-3 The effect of exhaust inlet temperatures and water flow rate on second law efficiency.*

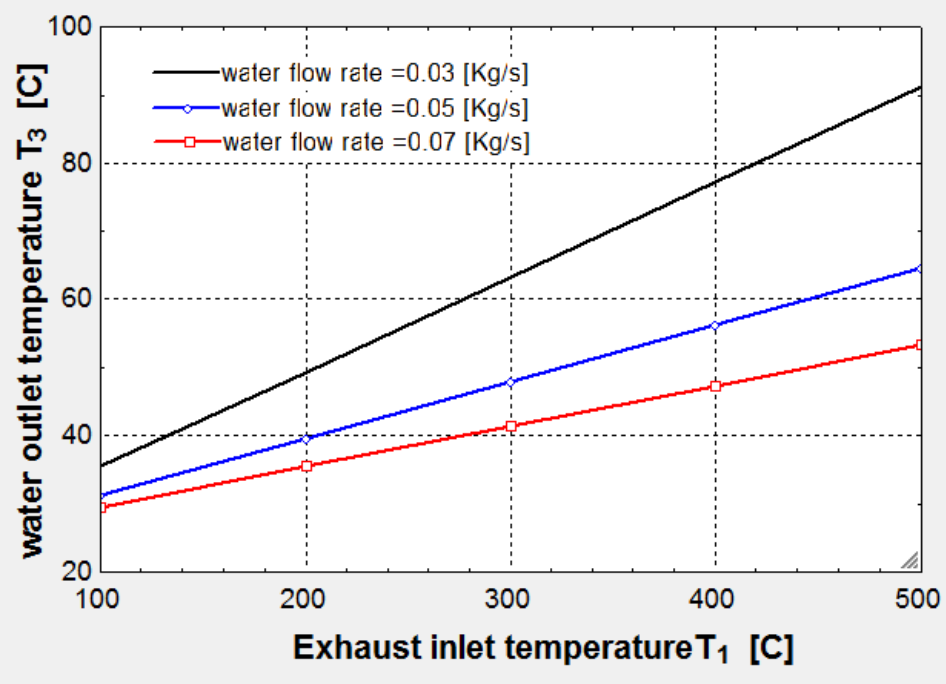


*Figure 4-4 The effect of exhaust inlet temperatures and water flow rate on water exit temperature.*

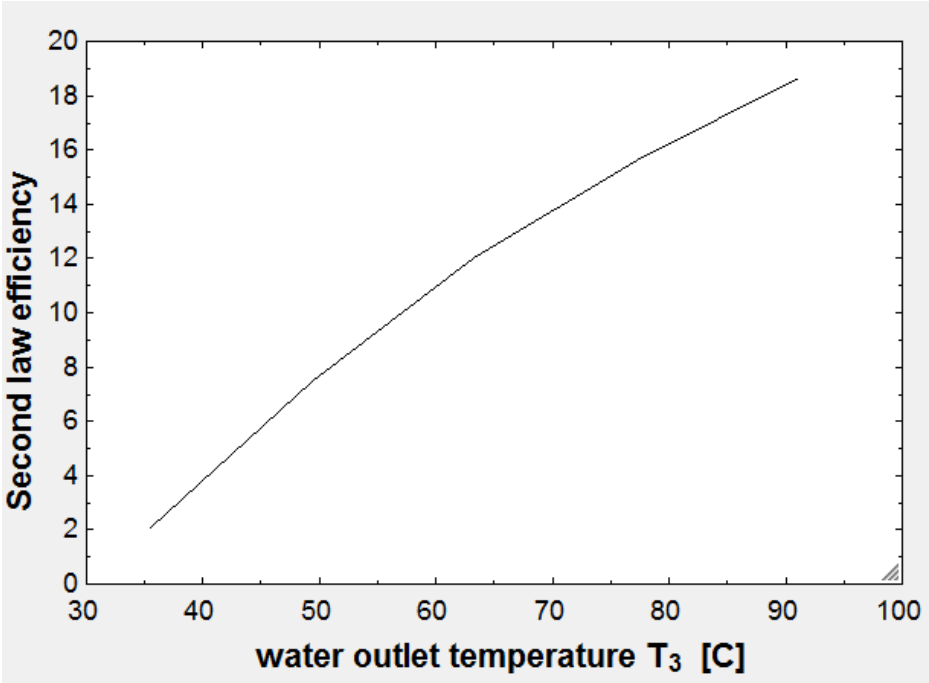


*Figure 4-5 Variation of second low efficiency with water exit temperature from heat exchanger.*

### 4.3 Conclusion

The exergy analysis was carried out for the system to see the effects of different variables on the second law efficiency and to know which parts of the system are responsible for most of exergy losses. Analysis showed that the second low efficiency of the system increases as the exhaust inlet temperature increase and decreases with the increase of water flow rate. analysis also showed that the heat exchanger alone is responsible for about 90% of the destructed exergy. At the second place comes the brine then the leaving exhaust is at the third place. These parts should then be the focus of future system improvements.

# Chapter 5: Cost analysis

## 5.1. Introduction

As Desalination plants consumes high rates of energy, and the prices of conventional types of energy isn't cheap and contributes largely to the cost of unit production [43] to [47], then it's vital to look for a solution for this problem. Since membrane distillation units works at relatively low temperature levels, so it's possible to use low grade energy with these units. In our work, we used a car engine exhaust to heat the feed water to the MD, bringing the distillation energy cost to zero. Banat et al. [48] performed an economic study to obtain an expectation for the water cost. According to their study, they calculated the cost of the produced water by the unit to be $15/m3. They found increasing the lifetime of the membrane and the lifetime of the plant will decrease the cost of producing fresh water. They stated that the desalination cost is a function of: quality of the feed water, plant capacity, cost of energy, pretreatment, investments amortization, process technology and plant life. Annual operating costs include membrane replacement costs, fixed charges and operating and maintenance costs.

If the decision of choosing the desalination unit was based on initial costs only, then the use of solar powered systems will be very limited. However, the advantage of using solar desalination systems is that they have negligible running energy costs. Costs per unit output from solar powered systems are relatively low when compared to the cost of alternative water resources

transported by trucks in isolated areas. Solar powered desalination systems remain one of the best options for water desalination in remote areas where there is no access to electric grids. Bouguecha et al [49] found that the total fixed costs for MD are $0.16–0.17/m3, compared to $0.25– 0.35/m3 for RO. Al-Obaidani et al [50] mentioned that the cost of unit production cost by a steam powered DCMD unit is 1.23 $/$m^3$, while the cost is reduced to 0.64 $/$m^3$ when using a low-grade energy instead of steam.

**5.2. Total unit production cost**

Desalination cost is a function of: pretreatment, feed water quality, energy cost, plant life time, plant capacity and process technology. The total cost per year of owing, maintaining and running a MD plant consists of: the amortization capital cost, membrane replacement cost and operating and maintenance cost.

**Capital cost**

Capital cost is the cost of system parts and installations. For our system, table 5.1 shows the cost of all system pats. From the above values, the total capital cost of the system is 866 $.

| Item | value |
|---|---|
| membrane | 13 $ |
| Membrane assembly | 106 $ |
| Heat Exchanger | 133 $ |
| Piping and fittings | 107 $ |
| Sensors | 400 $ |

| | |
|---|---|
| pump | 80 $ |
| tank | 27 $ |
| Total capital cost | 866 $ |

*Table 5-1 costs of system parts for a single stage AGMD, flat sheet membrane, channeled module.*

**Annual operating cost**

The annual operating cost consists of membrane replacement cost and operating and maintenance cost.

The rate of membrane replacement depends largely on the raw water. In our case, membrane replacement rate is once every three months.

The operating and maintenance costs includes mainly the costs of maintenance and spares. And it is estimated to be about 20 % of the system annual fixed cost.

**5.3. Results**

We first introduce amortization factor. It is the factor that is multiplied by the capital cost to calculate the annual fixed cost. And it is found from

$$a = \frac{i * (1+i)^n}{(1+i)^n - 1}$$

Where i is the interest rate and n is the system life time.

The annual fixed cost is

$$A_{fixed} = a * CC$$

Where CC is the capital cost.

The cost of membrane replacement is

$$A_{replacement} = 4 * membrane\ cost$$

And operating and maintenance is found from

$$A_{O\&M} = 0.2 * A_{fixed}$$

So, the total annual cost is

$$A_{total} = A_{fixed} + A_{replacement} + A_{O\&M}$$

Now, we will calculate the cost of unit product in ($/$m^3$)

$$A_{unit} = \frac{A_{total}}{f * M * 365}$$

Where f is system availability and M is the daily capacity of the system ($m^3$/day)

*Table 5-2 summarizes the results.*

| Item | value |
|---|---|
| **Capital cost** | 866 $ |
| **Interest rate** | 5% |
| **System life time** | 20 years |
| **Amortization factor** | 0.08024 |
| **System daily capacity** | 0.1 $m^3$/day |
| **System availability** | 1 (100%) |

| | |
|---|---|
| **Annual fixed cost** | 69.5 $ |
| **Annual operating and maintenance cost** | 13.9 $ |
| **Annual membrane replacement cost** | 52 $ |
| **Total annual cost** | 135.5 $ |
| **Cost of unit production** | 3.71 $\$/m^3$ |

Figures 5.1 and 5.2 shows the effect of variation of system life time and rate of membrane replacement on the cost of unit production. The cost is decreased as the life time of the system increased and it increases as the rate of replacing the membrane increases.

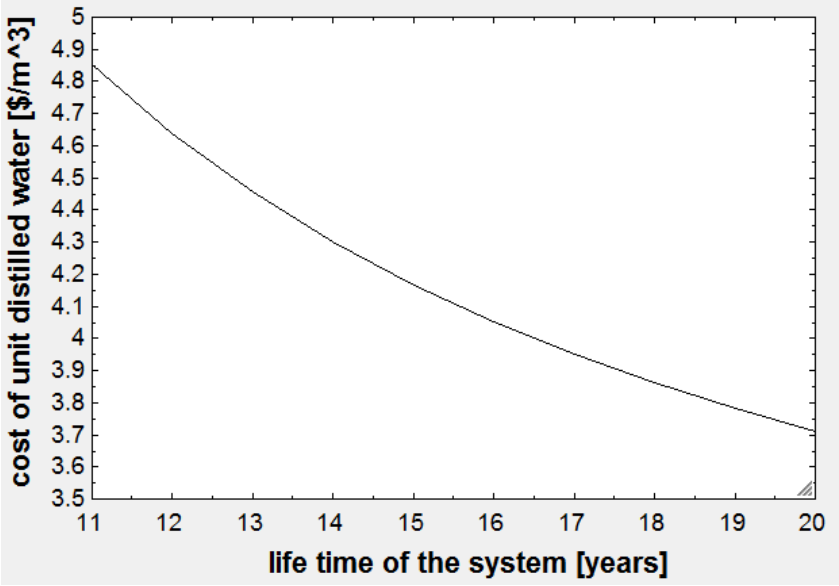


*Figure 5-1 Effect of life time of the system on unit production cost.*

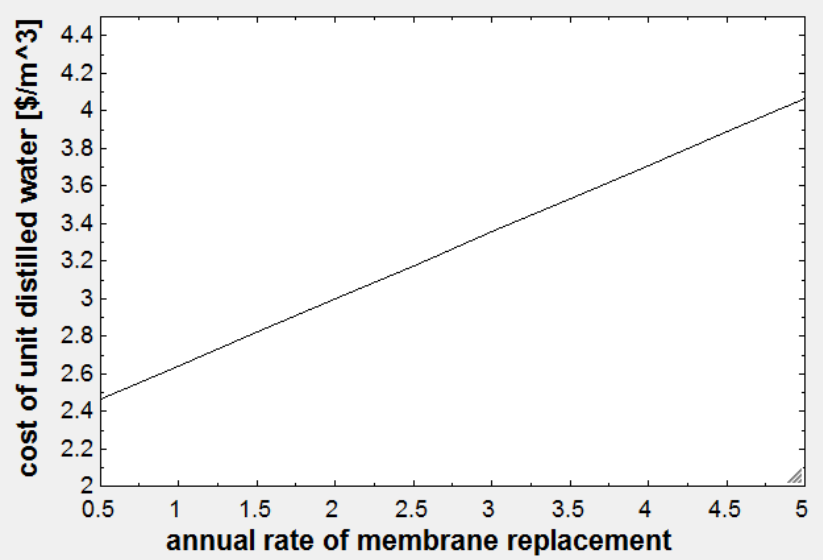


*Figure 5-2 Effect of annual rate of membrane replacement on unit production cost.*

**What if the engine is running specially to run the distillation system?**

In this case, we will take fuel cost into account as the engine is running only to run the MD system. The average specific fuel consumption of the engine was found experimentally to be 400 g/Kwh, which costs, according to fuel tariffs in Saudi Arabia, about 0.105$/KWh, and for 100 liters of daily capacity, and assuming the engine is running at average load and speed of 40 N.m and 2400 rpm.

Daily consumed energy = Torque * Speed * Time

$$= 40 * 2 * \pi * \frac{2400}{60} * 60 * 60 * 24 = 241.3 \text{ KWh}$$

Energy consumed per unit production = Daily consumed energy / Daily capacity

$$= 241.3/100 = 2.41 \text{ KWh}/m^3$$

Fuel cost per unit production = Energy consumed per unit production * Cost of KWh

$$= 2.41 * 0.105 = 0.253\$/m^3$$

Then, the total cost of unit production becomes = $0.253 + 3.71 = 3.96\$/m^3$

**5.4 Conclusion**

An economic analysis of the system was carried out to assess the cost of unit production cost, which was found to be $3.71\$/m^3$. Also, a parametric study was done to determine the effect of life time of the system and the rate of membrane replacement on the cost of unit production. The study shows that the unit production cost is decreased when the life time of the system is increased or when the rate of membrane replacement is decreased.

# Chapter 6: Conclusion and Recommendations

A full experimental study of an air gab membrane distillation module powered by the exhaust of a car engine was planned to be accomplished. A vision for the experimental setup that will achieve this mission was in mind and it was put into execution. A well-chosen heat exchanger type has gone through many design and fabrication phases until we reached the required output. Attached to a lab engine, the heat exchanger has shown a good ability of transferring heat between engine exhaust gases and feed water to the MD module reaching high temperatures of exit feed water from heat exchanger at the required feed water flow rates. The air gab membrane distillation module was then attached to the heat exchanger in addition to feed water tank, feed water pump, pressure gauges, thermometers and flow meters.

The experimental plan then was set to test the proposed system from all aspects and to clarify the effect of different variables like engine speed and load on system main parameters such as exhaust gases temperatures, feed water temperature and distillate flux.

Running the engine, the exhaust gases temperature starts to increase until it reaches a steady state temperature that is directly proportional to engine speed and load. With the increase in exhaust gases temperature, the feed water temperature also starts to increase gradually until it reaches a previously set value of 90 °C and then the system is turned off. The cooling water temperature was set to 33 °C with 4 l/min flow rate. As the feed water temperature increases, the distillate flux also increases. Increasing both engine load and speed causes an increase in

exhaust gases temperature, however it was noted that increasing engine load has a stronger effect on exhaust gases temperature than increasing engine speed.

Feed water temperature was found to increase with increasing engine load and speed due to the increase in exhaust gases temperature, and decrease with increasing feed water flow rate. The feed water temperature reached 90 °C after 20 minutes at 1 L/min feed water flow rate, while it reached the same temperature after 40 minutes at 3 L/min feed water flow rate at 2000 rpm and 30 N.m load. A test was made to observe the effect of opening the tank to atmosphere on feed water temperature for an open feed water cycle. It was found that the feed water temperature reached 90 °C after 80 minutes for an opened tank, while it took 160 minutes for the feed water temperature to reach 90 °C for a closed tank, which clarifies to how extent is the effect of opening the feed water tank to atmosphere and losing its heat to air by convection.

The distillate flux was found to increase with increasing engine load and speed, but again, increasing engine load had more significant effect on distillate flux than increasing engine speed, as distillate flux is directly proportional to feed water and exhaust gases temperatures. Distillate flux was also found to decrease with increasing feed water flow rate at the same engine load and speed. Also, distillate flux was increasing faster when the feed water tank was closed compared to open feed water tank. The average specific fuel consumption of the engine was 425 g/KW-h.

An exergy analysis was carried out for the system to know which parts are responsible for most of exergy destructions, so, it is an efficient tool for improvement and understanding of processes. An exergy analysis model was developed using EES software. The results show that the heat

exchanger alone is responsible for about 90% of the destructed exergy. At the second place comes the brine then the leaving exhaust is at the third place. The second low efficiency or exergy efficiency was found to increase with increasing feed water temperature.

Finally, an economic study was done to assess the feasibility of the proposed system. The cost of unit production was found to be 3.71 $/m3. It was also found that reducing the membrane replacement cost and increasing system life time has a significant positive effect on water production cost.

Going through the accomplished work and having a look at the obtained results, we can conclude that using waste heat to power desalination modules is becoming essential to provide an affordable potable water that also causes less harm to the environment. The system shows a good readiness to provide potable water using a portable system that only uses waste energy and by that the system contributes to saving energy resources, preserving the environment and reducing water production cost.

Future work should give attention to many points that helps improving the performance of the system and increasing its efficiency. A way to control the continuous increase of feed water temperature while running the engine should be obtained. This may include bypassing feed water away from heat exchanger when it reaches the desired value. Also, the optimum place of installing the heat exchanger relative to the engine should be investigated. Finally, the heat exchanger should be the focus of improvements regarding exergy efficiency as it was found to be

the major source of exergy destruction in the system. This will be done through eliminating second low losses as possible.

# Appendices

## Appendix A: EES code for heat exchanger design

```
mass_flow_rate = 2 [l/min] ; mass_flow_rate = 60*m_dot_water ; T_water_in = 25 [c] ;
T_water_out = 75 [c] ;" T_exhaust_in = 580 [c]  ;" rpm = 2000 [rpm] ;
D_inner_pipe = 0.0095 [m] ; Thickness = 0.001 [m] ; D_coil = 0.11 [m] ; D_outer_pipe = 0.2 [m] ;

"Analysis"

"Water"

Q = m_dot_water*cp_water*(T_water_out - T_water_in) ; "Heat transfered"

 C_cold = C_water

C_cold = m_dot_water*cp_water ; "Water heat capacity = Cold heat capacity"

 cp_water = 4180 [kJ/kg*c] ;


"Exhaust gas, for a 2000cc 4 stroke car engine"

m_dot_air = rho_air * displaced_volume * rpm * Eta_vol / ( 4 * 60 ) ;

 rho_air = 1.2 [kg/m^3] ;

 displaced_volume = 2000/10^6 [m^3] ;

 Eta_vol = 0.97 ;

 m_dot_exhaust = 1.06667 * m_dot_air ; "assuming fuel mass is about 10% of air mass"

 cp_exhaust = 1100 [kJ/kg*c] ;

 C_hot = C_exhaust ;

 C_hot = m_dot_exhaust * cp_exhaust ;   " Exhaust heat capacity = hot heat capacity"


"Design"

C_max = C_cold ;

 C_min = C_hot ;
```

"From energy balance"

C_hot * (T_exhaust_in - T_exhaust_out) = C_cold * (T_water_out - T_water_in) ;

"Effectiveness"

epsilon =Q/Q_max ;

Q_max = C_min * (T_exhaust_in - T_water_in) ;

"Heat Capacity Ratio"

C_r = C_min/C_max ;

"The Number of Transfer Units NTU"

"NTU = (-1/C_r )*ln(c_r*ln(1-epsilon) +1) ;" NTU=HX('crossflow_one_unmixed', epsilon, C_cold, C_hot, 'NTU') ;

" epsilon=HX('crossflow_one_unmixed', NTU, C_cold, C_hot, 'epsilon') ;"

"Overall heat transfer coefficient"

U = 1/((1/h_i) + (1/h_o)) ;

"For water inside the inner tube"

Re_D_internal = 4*m_dot_water/(3.14 * D_inner_pipe * water_viscosity) ;

water_viscosity = 0.000547 [Pa*s] ; "at average temperature of 50 C"

exhaust_viscosity = 0.0000235 [Pa*s] ; "at average temperature of 150 C"

"From Reynold number, the flow is turbulant"

Nu_D_internal = 0.023 * Re_D_internal^0.8 * Prandtl_number_water^0.4 ;

Prandtl_number_water = 3.6 ;

Nu_D_internal = h_i*D_inner_pipe/K_water ;

K_water = 0.625 ;

"For air outside the inner tube"

D_hydraulic = D_outer_pipe - D_coil ;

Re_D_external = 4*m_dot_exhaust*D_hydraulic/(exhaust_viscosity*3.14*(D_outer_pipe^2 - D_inner_pipe^2)) ;

"From Reynold's number, the flow is turbulant, The average heat transfer coefficient for cross-flow over a cylinder can be found from the

correlation presented by Churchill and Bernstein"

Nu_D_external = 0.3 + (0.62*Re_D_external^0.5*Prandtl_number_gas^0.3333)*(1+(Re_D_external/282000)^0.625)^0.8/(1+(0.4*Prandtl_number_gas)^0.667)^0.25 ;

Prandtl_number_gas = 0.69 ;

Nu_D_external = h_o*D_outer_inner_pipe/K_exhaust ;

D_outer_inner_pipe = 0.01 [m] ;

K_exhaust = 0.035 ;

"Estimating the heat transfer area and pipe length"

HeatTransferArea = NTU * C_min/U ;

PipeLength = HeatTransferArea/(3.14*D_average) ;

D_average = 0.01 [m] ;

## Appendix B: EES code for exergy analysis

```
"Mass flow rates" ; m_dot_1 = m_dot_exhaust  ; m_dot_2 = 0.05 [kg/s] ; m_dot_3 = m_dot_2  ; m_dot_4 = m_dot_exhaust  ; m_dot_5 = m_dot_exhaust  ; m_dot_6 = m_dot_2 - m_dot_8  ; m_dot_7 = m_dot_6 ;   m_dot_8 = 0.00025 [kg/s] ; m_dot_9 = m_dot_8 ;

"Exhaust gas temperatures" ;  T_0 = 25 [C] ; T_5 = 25 [C]  ;  T_1 = 500 [C] ;

"water Temperatures" ;  T_2 = 25 [C]  ; T_6 = T_3 - 2 [C] ; T_7 = 25 [C] ; T_8 = 30 [C] ; T_9 = 25 [C] ;


h_0 = h_0_w ; s_0 = s_0_w ;

"....."

m_dot_exhaust * Cp_exhaust * (T_1 - T_4)* Effectiveness = m_dot_3 * Cp_water * (T_3 - T_2) ;

Cp_water = 4180 [j/kg*k] ; Effectiveness = 0.8 ; Cp_exhaust = 1110 [j/kg*k] ;

C_water =  m_dot_3 * Cp_water ;

C_exhaust = m_dot_exhaust * Cp_exhaust ;

C_r = C_exhaust/C_water ;

A_h = 0.22 [m^2] ;

U = 96.31 [W/K*m^2] ;

NTU = U*A_h/C_exhaust ;


"from charts" Epsilon = 0.95 ;

q= Epsilon * q_max ;

q_max =  C_exhaust * (T_1 - T_2) ;

q = m_dot_exhaust * Cp_exhaust * (T_1 - T_4) ;

"....."

"Determining gas enthalpies"
```

h_0_e = 0.125*enthalpy(CarbonDioxide,T=T_0,P=P) + 0.1406*Enthalpy (Water , T=T_0 , P=P) + 0.7344* Enthalpy (Nitrogen, T=T_0, P=P) ;

h_1 = 0.125*enthalpy(CarbonDioxide,T=T_1,P=P) + 0.1406*Enthalpy (Water , T=T_1 , P=P) + 0.7344* Enthalpy (Nitrogen, T=T_1, P=P) ;

h_4 = 0.125*enthalpy(CarbonDioxide,T=T_4,P=P) + 0.1406*Enthalpy (Water , T=T_4 , P=P) + 0.7344* Enthalpy (Nitrogen, T=T_4, P=P) ;

h_5 = 0.125*enthalpy(CarbonDioxide,T=T_5,P=P) + 0.1406*Enthalpy (Water , T=T_5 , P=P) + 0.7344* Enthalpy (Nitrogen, T=T_5, P=P) ;

"Determining gas entropies"

s_0_e = (1/M_octane)*(M_CO2*Entropy (CarbonDioxide, T=T_0, P=P) - R*ln(Y_CO2) + M_N2*Entropy (Nitrogen, T=T_0, P=P) - R*ln(Y_N2) + M_H2O*Entropy (Water, T=T_0, P=P) - R*ln(Y_H2O)) ;

R = 8.314 [Kj/Kmol*K] ; Y_CO2 = 0.125 ; Y_N2 = 0.734 ; Y_H2O = 0.141 ; M_octane = 114.23 [Kg/Kmol] ; M_CO2 = 44 [Kg/Kmol] ; M_N2 = 28 [Kg/Kmol] ; M_H2O = 18 [Kg/Kmol] ;

s_1 = (1/M_octane)*(M_CO2*Entropy (CarbonDioxide, T=T_1, P=P) - R*ln(Y_CO2) + M_N2*Entropy (Nitrogen, T=T_1, P=P) - R*ln(Y_N2) + M_H2O*Entropy (Water, T=T_1, P=P) - R*ln(Y_H2O)) ;

s_4 = (1/M_octane)*(M_CO2*Entropy (CarbonDioxide, T=T_4, P=P) - R*ln(Y_CO2) + M_N2*Entropy (Nitrogen, T=T_4, P=P) - R*ln(Y_N2) + M_H2O*Entropy (Water, T=T_4, P=P) - R*ln(Y_H2O)) ;

s_5 = (1/M_octane)*(M_CO2*Entropy (CarbonDioxide, T=T_5, P=P) - R*ln(Y_CO2) + M_N2*Entropy (Nitrogen, T=T_5, P=P) - R*ln(Y_N2) + M_H2O*Entropy (Water, T=T_5, P=P) - R*ln(Y_H2O)) ;

"....."

"The following code requires the user to only enter the values of pressure, temperature, standard temperature (which is room or ambient temperature) and weight fraction of salt in saline water, respectively, in order to obtain enthalpy & entropy of saline water at any point"

P= 100 [Kpa] ;

"Solutions that have a concentration less than 5% are considered to be dilute solutions. Dilute solutions closely approximate the behavior of ideal solutions with negligible error since the effect of dissimilar molecules (water and salt) on each other is negligible. Brackish waters and

even seawaters have about 4% salinity at most, then they can be considered to be an ideal solutions."

"For ideal solutions the enthalpy and entropy of the mixture are the sum of the enthalpy and entropy of its individual components."

"The enthalpy of a component in a solution equals the enthalpy of that component when it existed alone as a pure substance at the mixture temperature and pressure. Therefore, the enthalpy of individual components does not change during mixing if they form an ideal solution."

"Enthalpy calculation of water and salt solution at T_0" ;

w_salt_0=0.00014 ;

h_0_w = w_salt_0*h_salt_0 + w_water_0*h_water_0 ;

h_salt_0 = Cp_salt*(T_0 + 273) ;

Cp_salt= 880 [j/kg*k] ;

h_water_0=Enthalpy(Water,T=T_0,P=P ) ;

"w_salt & w_water are the weight fractions of salt and water, respectively" ;

w_water_0 = 1 - w_salt_0 ;

"The entropy of a component in a mixture is always greater than the entropy of that component when it existed alone at the mixture temperature and pressure."

"Entropy calculation of water and salt solution at T_0"

s_0_w = w_salt_0*s_salt_pure_0 + w_water_0*s_water_pure_0 - R_water*(x_salt_0*ln(x_salt_0) + x_water_0*ln(x_water_0)) ;

R_water = 461.5 [j/kg*k] ;

s_water_pure_0 =Entropy(Water,T=T_0,P=P ) ;

s_salt_pure_0 = s_salt_standard + Cp_salt*ln((T_0+273)/(T_0+273)) ;

s_salt_standard = 1233.92 [j/kg*k] ; "satandard salt entropy" ;

"x_salt & x_water are the mole fractions of salt and water, respectively"

x_water_0 = w_water_0*M_mixture_0/M_water ;

x_salt_0 = 1 - x_water_0 ;

M_mixture_0 = 1/((w_water_0/M_water) + (w_salt_0/M_salt)) ; "mixture molar mass" ;

M_water = 18 [kg/kmol] ; "water molar mass" ;

M_salt = 58.44 [kg/kmol] ; "salt molar mass"

"Enthalpy calculation of water and salt solution at T_2" ;

w_salt_2 = 0.00014 ;

h_2 = w_salt_2*h_salt_2 + w_water_2*h_water_2 ;

h_salt_2 = Cp_salt*(T_2+273) ;

h_water_2=Enthalpy(Water,T=T_2,P=P ) ;

w_water_2 = 1 - w_salt_2 ;

"Entropy calculation of water and salt solution at T_2"

s_2 = w_salt_2*s_salt_pure_2 + w_water_2*s_water_pure_2 - R_water*(x_salt_2*ln(x_salt_2) + x_water_2*ln(x_water_2)) ;

s_water_pure_2 =Entropy(Water,T=T_2,P=P ) ;

s_salt_pure_2 = s_salt_standard + Cp_salt*ln((T_2+273)/(T_0+273)) ;

x_water_2 = w_water_2*M_mixture_2/M_water ;

x_salt_2 = 1 - x_water_2 ;

M_mixture_2 = 1/((w_water_2/M_water) + (w_salt_2/M_salt)) ;

"Enthalpy calculation of water and salt solution at T_3" ;

w_salt_3 = 0.00014 ;

h_3 = w_salt_3*h_salt_3 + w_water_3*h_water_3 ;

h_salt_3 = Cp_salt*(T_3+273) ;

h_water_3=Enthalpy(Water,T=T_3,P=P ) ;

w_water_3 = 1 - w_salt_3 ;

"Entropy calculation of water and salt solution at T_3"

s_3 = w_salt_3*s_salt_pure_3 + w_water_3*s_water_pure_3 - R_water*(x_salt_3*ln(x_salt_3) + x_water_3*ln(x_water_3)) ;

s_water_pure_3 =Entropy(Water,T=T_3,P=P ) ;

s_salt_pure_3 = s_salt_standard + Cp_salt*ln((T_3+273)/(T_0+273)) ;

```
x_water_3 = w_water_3*M_mixture_3/M_water ;

x_salt_3 = 1 - x_water_3 ;

M_mixture_3 = 1/((w_water_3/M_water) + (w_salt_3/M_salt))  ;

 "Enthalpy calculation of water and salt solution at T_6" ;

w_salt_6 = 0.0001447 ;

h_6 = w_salt_6*h_salt_6 + w_water_6*h_water_6 ;

h_salt_6 = Cp_salt*(T_6+273) ;

h_water_6=Enthalpy(Water,T=T_6,P=P ) ;

w_water_6 = 1 - w_salt_6 ;

 "Entropy calculation of water and salt solution at T_6"

s_6 = w_salt_6*s_salt_pure_6 + w_water_6*s_water_pure_6 - R_water*(x_salt_6*ln(x_salt_6)
+ x_water_6*ln(x_water_6)) ;

s_water_pure_6 =Entropy(Water,T=T_6,P=P ) ;

s_salt_pure_6 = s_salt_standard + Cp_salt*ln((T_6+273)/(T_0+273)) ;

x_water_6 = w_water_6*M_mixture_6/M_water ;

x_salt_6 = 1 - x_water_6 ;

M_mixture_6 = 1/((w_water_6/M_water) + (w_salt_6/M_salt))  ;

 "Enthalpy calculation of water and salt solution at T_7" ;

w_salt_7 = 0.0001447 ;

h_7 = w_salt_7*h_salt_7 + w_water_7*h_water_7 ;

h_salt_7 = Cp_salt*(T_7+273) ;

h_water_7=Enthalpy(Water,T=T_7,P=P ) ;

w_water_7 = 1 - w_salt_7 ;


"Entropy calculation of water and salt solution at T_7"

s_7 = w_salt_7*s_salt_pure_7 + w_water_7*s_water_pure_7 - R_water*(x_salt_7*ln(x_salt_7)
+ x_water_7*ln(x_water_7)) ;

s_water_pure_7 =Entropy(Water,T=T_7,P=P ) ;
```

```
s_salt_pure_7 = s_salt_standard + Cp_salt*ln((T_7+273)/(T_0+273)) ;

x_water_7 = w_water_7*M_mixture_7/M_water ;

x_salt_7 = 1 - x_water_7 ;

M_mixture_7 = 1/((w_water_7/M_water) + (w_salt_7/M_salt))  ;

 "Enthalpy calculation of water and salt solution at T_8" ;

w_salt_8 = 0.000004 ;

h_8 = w_salt_8*h_salt_8 + w_water_8*h_water_8 ;

h_salt_8 = Cp_salt*(T_8+273) ;

h_water_8=Enthalpy(Water,T=T_8,P=P ) ;

w_water_8 = 1 - w_salt_8 ;

 "Entropy calculation of water and salt solution at T_8"

s_8 = w_salt_8*s_salt_pure_8 + w_water_8*s_water_pure_8 - R_water*(x_salt_8*ln(x_salt_8)
+ x_water_8*ln(x_water_8)) ;

s_water_pure_8 =Entropy(Water,T=T_8,P=P ) ;

s_salt_pure_8 = s_salt_standard + Cp_salt*ln((T_8+273)/(T_0+273)) ;

x_water_8 = w_water_8*M_mixture_8/M_water ;

x_salt_8 = 1 - x_water_8 ;

M_mixture_8 = 1/((w_water_8/M_water) + (w_salt_8/M_salt))  ;

 "Enthalpy calculation of water and salt solution at T_9" ;

w_salt_9 = 0.000004 ;

h_9 = w_salt_9*h_salt_9 + w_water_9*h_water_9 ;

h_salt_9 = Cp_salt*(T_9+273) ;

h_water_9=Enthalpy(Water,T=T_9,P=P ) ;

w_water_9 = 1 - w_salt_9 ;

 "Entropy calculation of water and salt solution at T_9"

s_9 = w_salt_9*s_salt_pure_9 + w_water_9*s_water_pure_9 - R_water*(x_salt_9*ln(x_salt_9)
+ x_water_9*ln(x_water_9)) ;

s_water_pure_9 =Entropy(Water,T=T_9,P=P ) ;
```

s_salt_pure_9 = s_salt_standard + Cp_salt*ln((T_9+273)/(T_0+273)) ;

x_water_9 = w_water_9*M_mixture_9/M_water ;

x_salt_9 = 1 - x_water_9 ;

M_mixture_9 = 1/((w_water_9/M_water) + (w_salt_9/M_salt))  ;

"....."

"Calculating Exhaust gas flow rate, for a 2000cc 4-stroke car engine"

m_dot_air = rho_air * displaced_volume * rpm * Eta_vol / ( 4 * 60 ) ;

rpm = 2000 [rpm] ; rho_air = 1.2 [kg/m^3] ; displaced_volume = 2000/10^6 [m^3] ;

Eta_vol = 0.97 ; m_dot_exhaust = 1.0667 * m_dot_air ; "assuming fuel mass is about 10% of air mass"

"Second law efficiency calculations"

"Exergy input from exhaust to water" ; Ex_in = m_dot_1*(h_1 - h_0_e - (T_0+273)*(s_1 - s_0_e)) ;

"Minimum work of separation" ; W_dot_min = m_dot_6*(h_6-h_0-(T_0+273)*(s_6-s_0)) + m_dot_8*(h_8-h_0-(T_0+273)*(s_8-s_0)) ;

"Exergy destroyed" ; Ex_destroyd = Ex_in - W_dot_min ;

"Second law effeciency" ; Eta_II = (1 - (Ex_destroyd/Ex_in))*100 ;

"Percentage Exergy destroyed by each component"

"Percentage Exergy destroyed by heat exchanger" ;

Ex_destroyed_H.Ex_% = ( Ex_destroyed_H.Ex/Ex_in)*100 ;

Ex_destroyed_H.Ex = m_dot_1*(h_1 - h_0_e - (T_0+273)*(s_1 - s_0_e)) + m_dot_2*(h_2 - h_0 - (T_0+273)*(s_2 - s_0)) - m_dot_3*(h_3 - h_0 - (T_0+273)*(s_3 - s_0)) -  m_dot_4*(h_4 - h_0_e - (T_0+273)*(s_4 - s_0_e)) ;

"Percentage Exergy destroyed by leaving exhaust" ;

Ex_destroyed_leaving_exhaust_% = ( Ex_destroyed_leaving_exhaust/Ex_in)*100 ;

Ex_destroyed_leaving_exhaust = m_dot_4*(h_4 - h_0_e - (T_0+273)*(s_4 - s_0_e)) - m_dot_5*(h_5 - h_0_e - (T_0+273)*(s_5 - s_0_e)) ;

"Percentage Exergy destroyed by MD" ;

Ex_destroyed_MD_% = ( Ex_destroyed_MD/Ex_in)*100 ;

Ex_destroyed_MD = m_dot_3*(h_3 - h_0 - (T_0+273)*(s_3 - s_0)) - m_dot_6*(h_6 - h_0 - (T_0+273)*(s_6 - s_0)) - m_dot_8*(h_8 - h_0 - (T_0+273)*(s_8 - s_0)) ;

"Percentage Exergy destroyed by brine" ;

Ex_destroyed_brine_% = ( Ex_destroyed_brine/Ex_in)*100 ;

Ex_destroyed_brine = m_dot_6*(h_6 - h_0 - (T_0+273)*(s_6 - s_0)) - m_dot_7*(h_7 - h_0 - (T_0+273)*(s_7 - s_0)) ;

## References

1. Kanae T. Oki, S. Global Hydrological Cycles and World Water Resources. Science Vol 313, Issue 5790, 25 August 2006.

2. Rijsberman Frank R. Water scarcity: Fact or fiction? Agricultural Water Management 80 (2006) 5–22

3. AL-RASHED M. F, M. M. SHERIF. Water Resources in the GCC Countries: An Overview. Water Resources Management 14: 59–75, 2000.

4. DeNicola Erica, MS, Omar S. Aburizaiza, Azhar Siddique, Haider Khwaja, David O. Carpenter. Climate Change and Water Scarcity: The Case of Saudi Arabia. VOL. 81, NO. 3, 2015 ISSN 2214-9996

5. Alklaibi A. M, N. Lior. Membrane-distillation desalination: status and potential. Desalination 171 (2004) 111-131.

6. Gonzáleza Daniel, José Amigoa, Francisco Suáreza. Membrane distillation: Perspectives for sustainable and improved desalination. Renewable and Sustainable Energy Reviews 80 (2017) 238–259.

7. Rahimi Bijan, Hui Tong Chua. Chapter 1: Introduction to Desalination. Low Grade Heat Driven Multi-Effect Distillation and Desalination, 2017, Pages 1-17.

8. Loutatidou Savvina, Musthafa O. Mavukkandy, Sudip Chakraborty, Hassan A. Arafat. Chapter 1: Introduction: What is Sustainable Desalination? Desalination Sustainability, 2017, Pages 1-30.

9. Zheng Hongfei. Chapter 1: General Problems in Seawater Desalination Solar Energy Desalination Technology, 2017, Pages 1-46.

10. Belessiotis Vassilis, Soteris Kalogirou, Emmy Delyannis. Chapter One: Desalination Methods and Technologies—Water and Energy. Thermal Solar Desalination, 2016, Pages 1-19.

11. Sanmartino Julio A, Mohamed Khayet, M.C. García-Payo. Chapter 4: Desalination by Membrane Distillation. Emerging Membrane Technology for Sustainable Water Treatment, 2016, Pages 77-109.

12. Younos T, Kimberly E. Tulou. Overview of Desalination Techniques. Journal of contemporary water research & education issue 132, pages 3-10, December 2005.

13. Subramani Arun, Joseph G. Jacangelo. Emerging desalination technologies for water treatment: A critical review. water research 75 (2015) 164 e187.

14. Alkhudhiri A, N. Darwish, N. Hilal. Membrane distillation: A comprehensive review. Desalination 287 (2012) 2–18.

15. Lawson W, R. Lloyd. Membrane distillation. Journal of Membrane Science 124 (1997) 1-25.

16. Alklaibi A. M, Noam Lior. Membrane-distillation desalination: status and potential. Desalination 171 (2004) 111-131.

17. El-Bourawi M. S, Z. Ding, R. Ma, M. Khayet. A framework for better understanding membrane distillation separation process. Journal of Membrane Science 285 (2006) 4–29.

18. Lawson W, R. Lloyd. Membrane distillation. II. Direct contact MD. Journal of Membrane Science 120 (1996) 123-133.

19. Lawson W, R. Lloyd. Membrane distillation. I. Module design and performance evaluation using vacuum membrane distillation. Journal of Membrane Science 12(1 (1996) 1 I 1-121.

20. Godino P, Luis Pefia, Juan I. Mengual. Membrane distillation: theory and experiments. Journal of Membrane Science 121 (1996) 83-93.

21. SMOLDERS K. and A.C.M. FRANKEN. Terminology for Membrane Distillation. Desalination, 72 (1989) 249-262.

22. Gostoli C and G.C. Sarti. Separation of liquid mixtures by membrane distillation. Journal of Membrane Science, 41 (1989) 211-224.

23. Rasool M, F. Banat. Desalination by solar powered membrane distillation systems. Desalination 308 (2013) 186–197.

24. Hogan P, A. Sudjito, G. Fane, G. Morrison, Desalination by solar heated membrane distillation, Desalination 81 (1991) 81–90.

25. Thomas K. Overview of village scale, Renew. Energy Powered Desalination (1997) pp. 1–31 (NREL/TP-440-22083, UC Category: 1210 DE 97000240).

26. Xu Y, B. k. Zhu, Y. Y. Xu Pilot test of vacuum membrane distillation for seawater desalination on a ship. Desalination 189 (2006) 165–169.

27. Khalifa A. E, D. U. Lawal, M. Antar. performance of air gap membrane distillation unit for water desalination. IMECE2014-36031.

**28. Chunhua Qi, Lv Hongqing, Feng Houjun, Lv Qingchun, Xing Yulei. Performance and economic analysis of the distilled seawater desalination process using low-temperature waste hot water. Applied Thermal Engineering. Volume 122, 25 July 2017, Pages 712-722.**

29. Dastgerdi Hamid, Peter B Whittaker, Hui Tong Chua. New MED based desalination process for low grade waste heat. 395- 10.1016/j.desal.2016.05.022.

30. Lokarea Omkar, Sakineh Tavakkolia, Gianfranco Rodriguezb, Vikas Khannaa, Radisav Vidica. Integrating membrane distillation with waste heat from natural gas compressor stations for produced water treatment in Pennsylvania. Desalination, Volume 413, 1 July 2017, Pages 144–153.

31. Shirazi M. A, A. Kargari & M. A. Shirazi (2012) Direct contact membrane distillation for seawater desalination, Desalination and Water Treatment, 49:1-3, 368-375, DOI: 10.1080/19443994.2012.719466.

32. Schofield R.W, A.G. Fane, C.J.D. Fell and R. Macoun. Factors Affecting Flux in Membrane Distillation. Desalination, 77 (1990) 279-294.

33. Khalifa A, D. Lawal, M. Antar, M. Khayet. Experimental and theoretical investigation on water desalination using air gap membrane distillation. Desalination 376 (2015) 94–108.

34. Khalifa A. E. M. A. Antar, M. S. Farag. Experimental and Theoretical Comparative Study of Performance and Emissions for a Fuel Injection SI Engine with Two Octane Blends. Arab J Sci Eng.DOI 10.1007/s13369-015-1649-2.

35. Costa V.A.F. On the exergy balance equation and the exergy destruction. Energy Volume 116, Part 1, 1 December 2016, Pages 824-835.

36. Ali Emad. Energy efficient configuration of Membrane Distillation units for brackish water desalination using exergy analysis Chemical Engineering Research and Design, Volume 125, September 2017, Pages 245-256.

37. Carrasquer Beatriz, Amaya Martínez-Gracia, Javier Uche. Exergy costs analysis of water desalination and purification techniques by transfer functions. Energy Conversion and Management, Volume 126, 15 October 2016, Pages 51-59.

38. Fitzsimons Lorna, Brian Corcoran, Paul Young, Greg Foley. Exergy analysis of water purification and desalination: A study of exergy model approaches. Desalination, Volume 359, 2 March 2015, Pages 212-224.

39. Karan John H, H. Mistry, Mostafa H. Sharqawy, Gregory P. Thiel. Chapter 4: Thermodynamics, Exergy, and Energy Efficiency in Desalination Systems. Desalination Sustainability, 2017, Pages 127-206.

40. Ghamdi Ahmed Al, Ibrahim Mustafa. Exergy analysis of a MSF desalination plant in Yanbu, Saudi Arabia. Desalination, Volume 399, 1 December 2016, Pages 148-158.

41. Deniz Emrah, Serkan Çınar. Energy, exergy, economic and environmental (4E) analysis of a solar desalination system with humidification-dehumidification. Energy Conversion and Management, Volume 126, 15 October 2016, Pages 12-19.

32. Banat F, N. Jwaied. Exergy analysis of desalination by solar-powered membrane distillation units. Desalination Volume 230, Issues 1–3, 30 September 2008, Pages 27-40.

43. Pinto F. Silva, R. Cunha Marques. Desalination projects economic feasibility: A standardization of cost determinants. Renewable and Sustainable Energy Reviews, Volume 78, October 2017, Pages 904-915.

44. Papapetrou Michael, Andrea Cipollina, Umberto La Commare, Giorgio Micale, George Kosmadakis. Assessment of methodologies and data used to calculate desalination costs. Desalination, Volume 419, 1 October 2017, Pages 8-19.

45. Kim In S, Moonhyun Hwang, Changkyoo Choi. Chapter 2: Membrane-Based Desalination Technology for Energy Efficiency and Cost Reduction. Desalination Sustainability, 2017, Pages 31-74.

46. Wittholz Michelle K, Brian K. O'Neill, Chris B. Colby, David Lewis. Estimating the cost of desalination plants using a cost database. Desalination, Volume 229, Issues 1–3, 15 September 2008, Pages 10-20.

47. Ang W.L, D. Nordin, A.W. Mohammad, A. Benamor, N. Hilal. Effect of membrane performance including fouling on cost optimization in brackish water desalination process. Chemical Engineering Research and Design, Volume 117, January 2017, Pages 401-413.

48. Banat, N. Jwaied. Economic evaluation of desalination by small-scale autonomous solar powered membrane distillation units. Desalination 220 (2008) 566-573.

49. Bouguecha S, B. Hamrouni and M. Dhahabi, Small scale desalination pilots powered by renewable energy sources: case studies, Desalination, 183 (2005) 165–151.

50. Al-Obaidania Sulaiman b, Efrem Curcio, Francesca Macedoniob, Gianluca Profiob,

51. Al-Hinaid Hilal, Enrico Drioli. Potential of membrane distillation in seawater desalination: Thermal efficiency, sensitivity study and cost estimation, Journal of Membrane Science 323 (2008) 85–98.

# Vitae

Name: Abdelrahman Abdelsalam Etman

Nationality: Egyptian

Date of birth: 20-Feb 1989

Email: emeabdelrahman@yahoo.com

Address: 28th Taawonyat Semouha, Alexandria, Egypt.

Academic background: B.Sc. in Electromechanical engineering. Alexandria University.